Transactions

R R F M 2009

Vienna, Austria
22 -25 March 2009

Session IV

Innovative Methods in Research Reactor Physics

TRIGA FUEL BURN-UP CALCULATIONS SUPPORTED BY GAMMA SCANNING

R.KHAN, S.KARIMZADEH, H.BÖCK, M.VILLA

Vienna University of Technology/Atominstitute
Stadion allee 2, A-1020, Vienna, Austria

High resolution gamma-ray spectroscopy based non-destructive methods is employed to measure spent fuel parameters. By this method, the axial distribution of Cesium-137 has been measured which results in an axial burn up profiles. Knowing the exact irradiation history of the fuel, four spent TRIGA fuel elements have been selected for on-site gamma scanning using a special shielded scanning device developed at the Atominstitute. Each selected fuel element was transferred into the fuel inspection unit using the standard fuel transfer cask. Each fuel element was scanned in one centimetre steps of its active fuel length and the Cesium-137 activity was determined as a proved burn up indicator. The absolute activity of each centimetre was measured and compared with the reactor physics code ORIGEN2.2 results. This code was used to calculate average burn up and isotopic composition of fuel element. The comparison between measured and calculated results shows good agreement.

1   Introduction

The Atominstitute of the Austrian Universities (ATI) operates a TRIGA Mark II research reactor since March 1962 with thermal power of 250 kW. The current TRIGA core is a mixed core of three types of U-ZrH TRGA fuel i.e. 102 type with aluminium clad, 104 type with stainless steel clad and 110 type or FLIP fuel elements (FEs) [1]. The current core consists of 82 FEs. Out of 82, 52 elements are 102 type, 21 are 104 types while remaining 9 are 110 type or FLIP FE. Only 102-type (Al-clad) FEs were taken in this paper which is composed of 20% enriched U-ZrH$_{1.0}$ fuel, with 8.5 wt. % U content. The average material and dimensional specifications (grams and cm) of 102-type typical FE are given in Table 1.

Length of fuel meat (cm)	35.60	U-235 (g)	36.13
Diameter of fuel meat (cm)	3.59	U-238 (g)	146.03
Graphite reflector length (cm)	10.21	U-234, U-236 (g)	0.36
Cladding thickness (cm)	0.076	Al-clad (g)	163.00
Burnable poison (cm)	2- SmO$_3$-disks	Zr-H (g)	2066.06

Tab 1: Material and dimensional specifications of 102-fuel elements

The burn up (BU) indicates the useful lifetime of fuel in the reactor core and is a measure of the total amount of thermal energy generated per unit quantity of heavy element (U) charged to the core. Usually burn-up is expressed in MW d / (kg U) [2]. As the Cs-137 intensity is proportional to burn up [2], therefore the main efforts of this work were focused on

1. An average burn-up and isotopic composition calculation for four selected irradiated FEs employing ORIGEN2.2 reactor physics code
2. Confirmation of calculations by the method of high-resolution gamma spectroscopy
3. Axial redistribution of the burn-up applying gamma spectrometric measurements.

This series of measurements was carried out for four 102-type type FEs i.e. FE: 2124, FE: 2196, FE: 2156 and FE: 2077. The only difference between these FEs was their individual irradiation histories and the resulting burn up. Typical Aluminium clad FE is shown in figure 1.

Keeping all factors of accuracy in view, the FE 2196 was identified with the simplest irradiation history [1]. Using Full Power Days (FPD) from the log books [6], the Full Operating Length (FOL) in days and power at FOL in MW was calculated for each selected FE to input the ORIGEN2.2 for BU and isotopic composition calculation. These calculations for the representative FE 2196 are shown in table 2. The average power at FOL was calculated as 0.34773 kW.
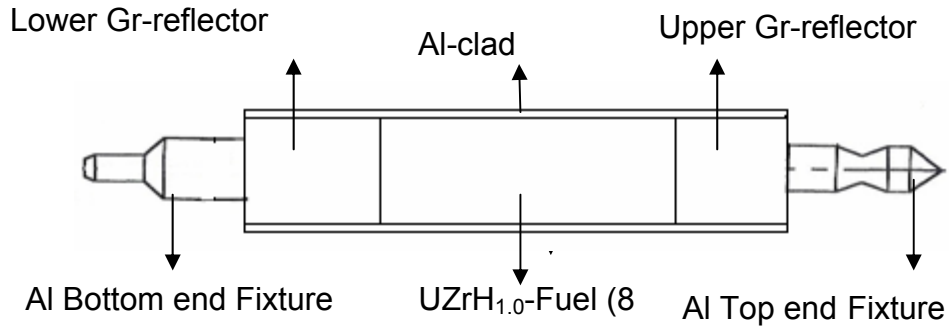
Fig 1: Typical aluminium clad fuel element

From	To	FE Position	Burn up (MWD)	FPD (Days)	FOL (days)	MW at FPD	MW at FOL
07.03.1962	27.07.1964	B04	4.132	41.322	872	1.451×10^{-3}	$6,879 \times 10^{-5}$
28.07.1964	07.08.1970	B04	69.504	278.016	2202	3.629×10^{-3}	4.582×10^{-4}
08.08.1970	06.11.2008	Out	0	0	0	0	0

Tab 2: Irradiation history calculations from log book for typical FE: 2196

The irradiation history of the FE 2196 in terms of FOL (days) and average power (MW$_{Th}$) at Full Length, is shown in the figure 2. The current Cs-137 radioactivity (Bq) of each FE was calculated under the given irradiation history. This fuel element was also measured by gamma spectroscopy. These measurements were performed for each centimetre of the selected FE. The measurement results were found close enough to calculations, confirming the ORIGEN2.2 model for burn up and isotopic composition computation. Applying the measured axial distribution of the Cs-137, the relative axial burn up of each centimetre for the selected fuel elements has been included in this work.
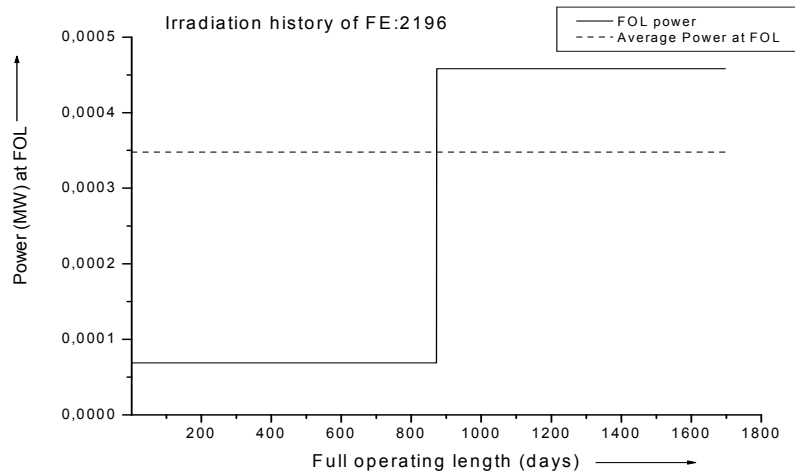

Fig 2: Irradiation history of each fuel element at full operating length (FOL)

2   Methodology

2.1   Gamma Spectroscopy

The measurements were performed in the reactor hall of ATI outside the reactor shield with an adequate shielding by the lead fuel transfer cask and the lead shield of the fuel inspection unit. The experimental setup consists of fuel transfer cask, inspection unit, beam collimator and coaxial high purity germanium p-type detector (HPGe) has been shown in the figure 3.

2

The relative efficiency as performance parameter of the HPGe was 15%. The fuel element to be measured was mounted to fuel inspection unit through fuel transfer cask where it can be moved vertically with an adjustable speed. The axial position of the FE to be measured is indicated by a digital monitor fixed on the elevator system. Although this unique fuel elevator system has the ability to scan each millimetre of the fuel element accurately but conveniently one centimetre was selected for each measurement. The collimator of 1 cm diameter was used and the distance between detector and fuel rod was kept about 10 cm. The counting errors were controlled up to 1.0% (in one standard deviation). The counting dead times were in generally controlled to be ≤20% corrected automatically during the counting period.

Using suitable fast electronics, the 300 seconds recorded gamma ray spectrum for each centimetre of FE was acquired and saved on a removable hard disk of the PC for further detailed analysis. Figure 4 shows a typical gamma ray spectrum with Cs-137 peak. The spectrum analysis resulted in the counts per second of Cs-137 (net peak area) which gives experimental activity using following relation [5].

$$A_{\exp} = \frac{C}{\varepsilon \cdot \gamma \cdot f}$$

Where "C" is Photo peak area (cps), "ε" is Absolute efficiency (%), "γ" is Gamma ray branching ratio and "f" is fuel self attenuation factor (%).
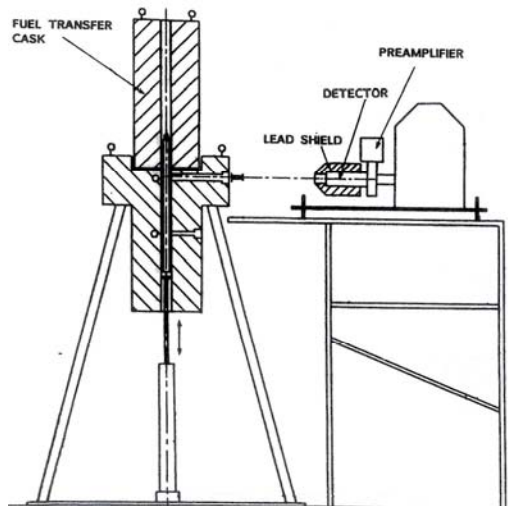

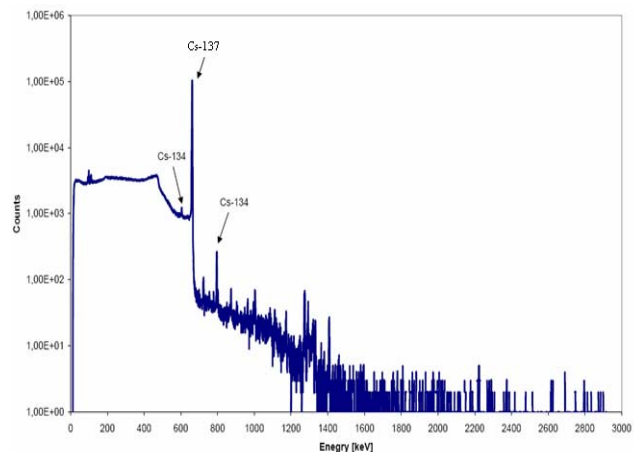Fig 3: Fuel inspection unit   Fig 4: The typical gamma spectrum 102-FE

2.1.1 Self shielding factor calculation

The correction (self-shielding factor "f") for the fraction of those gamma-rays being absorbed by the fuel has been calculated employing MCNP5 [3]. In this case this factor was found as 15% of total Cs-137.

2.2 *Reactor Physics Calculations*

ORIGEN2.2 is an ORNL isotope generation and decay code and selected for activity and TRIGA spent fuel isotopic composition calculations [4]. These calculations require: the initial compositions (table1), One-group microscopic cross-sections for each isotope [4], material feed and removal rates, the length of the irradiation periods (from log books) and the flux or power of the irradiation.

The ORIGEN2.2 fission cross section and fission product yield libraries for TRIGA fuel either has not been developed or it is not known if any one existed. Therefore in this work, 102-type TRIGA fuel elements were modelled using available cross-section and fission product yield libraries. Theses calculations used the standard burn up PWR libraries for TRIGA reactor.

All described fuel elements were calculated separately because of their different irradiation history. The irradiation power of each FE at some specific location was calculated by relation given below [7]:

$$P_{irr} = \frac{Total\ Thermal\ Power}{Number\ of\ FE}\ x\ P_f$$

Where total thermal power of TRIGA Vienna is 250 kW and P_f is power factor .The values of P_f are 1.0, 0.9, 0.8, 0.7, 0.6, 0.5 and 0.5 for A, B, C, D, E, F and G ring of the core respectively.

3 Results and Discussions

The comparison of calculated and measured results has been given in table3 & figure 5. The reasons these deviations between have been discussed in this section one by one.

FE number	Burn up (MWh)	Cal. Activity (Bq) Cs-37/cm	Meas. Activity (Bq) Cs-137/cm	Percent difference (%))
2196	25,68	1.351E+09	1.362E+09	0.8200
2077	30,912	1.715E+09	1.597E+09	6.8790
2156	58,08	3.519E+09	3.600E+09	2.2979
2124	69,24	4.588E+09	4.440E+09	3.2127

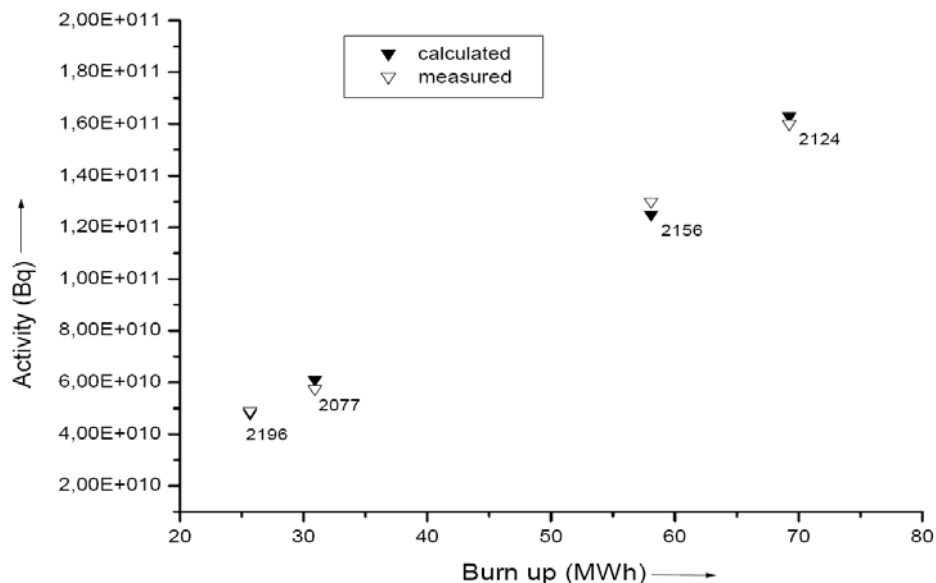Tab 3: Comparison between Calculated and measured results

Fig 5: Comparison of ORIGEN2 calculations and gamma spectroscopic measurement

First, the reactor has been operating since 1974 with mixed core, using three different types of fuel elements. Due to the mixed core composition, the accuracy of calculated burn-up varies significantly from element to element [1]. Second, the basis of the calculation (i.e. MWD) was taken from log books and because of long history of the fuel elements since 1962; some operational uncertainties in the log books may cause these variations in the accuracy. Third, the PWR libraries of ORIGEN2.2 have been used for this TRIGA fuel element model which have its own contribution in these deviations for example, it can also be seen in figure 5 that with increasing the burn up, difference between calculations and measurements increases showing that PWR library for TRIGA reactors is well valid in lower burn up regions.

The spectrometric analysis provides the Cs-137 axial distribution for given fuel elements. As mentioned that Cs-137 production is proportional to BU therefore applying this axial distribution of Cs-137, the axial burn-up distribution of each measured TRIGA fuel element can be predicted with reasonable accuracy.

4

To estimate the axial relative bun up for each centimetre of the FE, the constant conversion factor has been calculated. In our case, this factor was different for each measured fuel elements. This conversion factor provides the relation between activity and BU for TRIGA fuel element. Both measured Cs-137 and implied (predicted) burn up axial distribution for FE: 2196 have been shown in the figure 6. Two slight peaks at the top and bottom end of each fuel meat indicate two axial graphite reflectors i.e. upper and lower reflector as shown in figure 1.
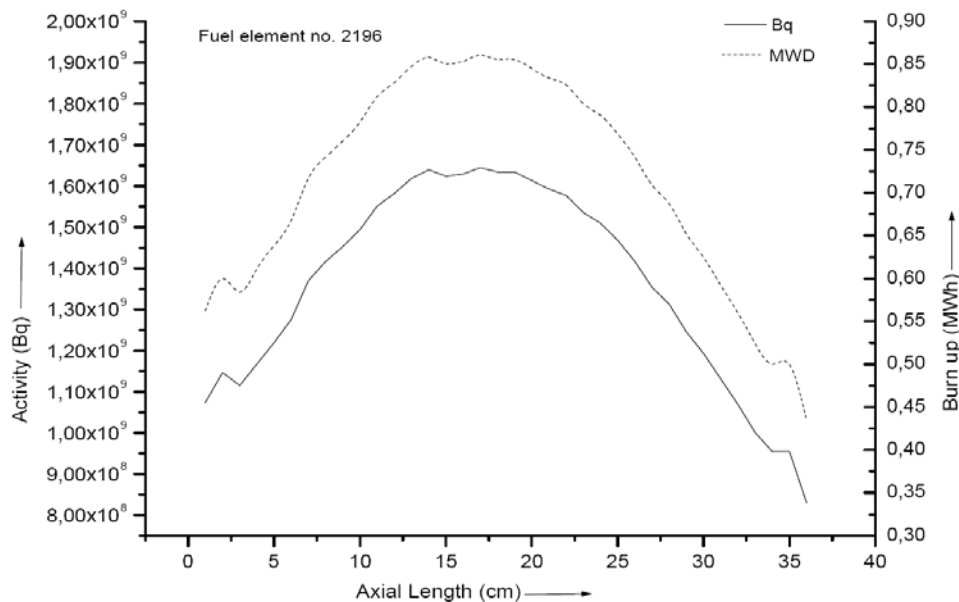

Fig 6: The measured Cs-137 and implied axial burn up distribution of FE 2196

Conclusions

ORIGEN2.2 software has been applied to TRIGA reactors for average fuel burn up using PWR library. Employing the Cs-137 axial distribution, the axial burn up of same fuel element has been predicted for each scanned segment of fuel element. The high resolution gamma spectroscopy technology that has been developed is versatile measuring method. It provides rapid information about several processes taking place in the fuel meat with the possibility of feedback to operators.

References

[1] M. Ravnik, M. Strebl, H. Böck and I. Mele " Determination of the burn-up of TRIGA fuel element by calculation and reactivity experiments" Carl Hanser, München 1992.

[2] Matsson and B. Grapengiessew "Developments in Gamma Scanning of Irradiated Nuclear Fuel" Pergamon journal 1997.

[3] Monte Carlo Team, "MCNP – A General Monte Carlo N-Particle Transport Code, Version 5", LA-UR-03-1987, Los Alamos National Laboratory, April 24, 2003.

[4] S. Ludwig, "Revision to ORIGEN2 – Version 2.2," Oak Ridge National Laboratory, May 23, 2002.

[5] Tien-Ko Wanga, Jinn-Jer Peir "An iterative approach for TRIGA fuel burn-up determination using nondestructive gamma-ray spectrometry", Applied Radiation and Isotopes 52 (2000) 105±118.

[6] Log books of TRIGA Mark II, Vienna, Austria

[7] A. Persic, M. Ravnik, S. Slavic, T.Zager " TRIGLAV A Program package for Research Reactor Calculations", IJS-DP 7862, ver. 1, March 2000.

ANALYSIS OF NEW SAFETY CRITERIA FOR CABRI REACTOR CORE

D. BLANC, S. PIGNET, F. ECRABET

Reactor Safety Division, Institut de Radioprotection et de Sûreté Nucléaire (IRSN)
31, Avenue de la Division Leclerc
92260 Fontenay-Aux-Roses - France

V. GEORGENTHUM, A. MOAL

Major Accident Prevention Division, Institut de Radioprotection et de Sûreté Nucléaire (IRSN)
BP 3
13115 Saint-Paul-lez-Durance Cedex - France

ABSTRACT

As the technical support of the French Safety Authority, IRSN has examined the new criteria proposed by the operator of the CABRI reactor to insure the clad integrity of the driver core fuel rods during fast reactivity insertion transients. The main issues of the extensive analysis of the clad failure phenomena and of the additional justifications on the choice of the strain limit are presented and discussed. The evaluation of the methodology to compute the thermo-mechanical behaviour of the fuel rods (based on the use of the SCANAIR code) is comprehensively described. The main results of a complementary study aimed at comparing the energy deposit required to match the criteria proposed for CABRI with those leading to failures in SPERT-CDC (USA) and NSRR (Japan) experiments are also presented. As the operator has included in the safety demonstration all the additional requirements identified by IRSN, it can be concluded that the present safety demonstration is sufficiently robust and guarantees the absence of rod failure during fast transients.

1. Introduction

The CABRI reactor is located on the French Commissariat à l'Energie Atomique (CEA) site at Cadarache. This reactor is used to simulate a reactivity initiated accident on an experimental fuel rod. The reactor includes:

- a driver core with a nominal power of 25 MW, cooled with water in forced convection. This driver core includes slightly enriched fuel rods (6% in U_{235}) and a stainless cladding material,
- an experimental loop, with its own cooling system. A part of this loop is located at the centre of the driver core and contains the instrumented test device with the experimental fuel rod.

Since 1978, the CABRI reactor has been mainly devoted to the study of fast breeder reactors (FBR) fuel behaviour. So, the coolant contained in the experimental loop was sodium. At the beginning of the years 2000, it was decided to replace the experimental sodium-cooled loop by a pressurised water loop able to recreate the thermal-hydraulic conditions of a pressurized water reactor (PWR) i.e. a 15.5 MPa pressure and a temperature between 280°C and 320°C.

For the previous tests simulating a fast reactivity insertion, the clad integrity of the driver core fuel rods was insured by the following safety criteria: the clad-to-coolant heat flux must not exceed 750 $W.cm^{-2}$, deemed a conservative value of the critical heat flux. CEA has recalculated some previous tests and have found that the value of 750 $W.cm^{-2}$ was exceeded in several cases. The calculations for the forecasted tests with the new experimental loop gave the same results. So CEA proposed a new approach in order to insure driver core fuel rods clad integrity during the forecasted reactivity transients.

IRSN acts as a technical support (TSO) of the French Nuclear Safety Authority (ASN). In the scope of the CABRI reactor restart, IRSN has examined the new criteria proposed by CEA.

2. CABRI driver core new safety criteria

The new safety approach of CEA is based on the study of the driver core fuel rods behaviour during fast reactivity insertion transients. The objective of this study is to check the mechanical strength of these rods taking into account the clad temperature transient and including a possible transient dry out around some fuel claddings.

This safety approach is based on the three following criteria:

- the maximum clad temperature must be lower than 1300°C to prevent clad from melting (the melting temperature of the stainless steel cladding material is in the range of 1450°C),
- the clad strain must be lower than 3.65% to prevent from ductile rupture; this value is 50% of the rupture elongation measured on samples representatives of the clad,
- fuel pellets melting must be avoided.

During the technical discussions between IRSN and CEA, different methodologies able to simulate fast reactivity insertion transients were examined and it appeared to IRSN that the SCANAIR code was well adequate for this purpose (see § 4). The calculations include a set of conservative hypotheses established for each criterion and the calculations results are compared to the above criteria.

3. Assessment of the new criteria
3.1 Phenomenology of clad degradation

CEA considered only two clad failure mechanisms: clad melting (associated to the first criterion) and the ductile rupture (associated to the second criterion). IRSN reviewed other phenomena able to degrade the clad and focused its attention to the following three items.

Thermal creep
During fast reactivity transients, there is a first phase during which the fast increase of the fuel temperature leads to pellet-clad mechanical interaction (PCMI) with a risk of ductile rupture. When the power has decreased, the pellet-to-clad gap re-opens due to the fuel pellets contraction. Then, the internal gas pressure is about 0.6 MPa and the clad temperature can reach 1270°C during a few seconds. IRSN raised the issue of the thermal creep failure risk and the CEA's answer consisted in presenting the following results coming from tests specially performed for CABRI rods in the EDGAR experimental loop:
- a clad sample was pressurized by gas at a pressure of 0.95 MPa with a temperature of 1200°C during 1100s before the tube broke,
- another clad sample was maintained during 10s at 1290°C without any deformation or rupture.

Oxidation
IRSN considered that there is an increase of the failure risk due to oxidation when the clad temperature reaches 1200°C. For this topic, CEA showed that the first EDGAR test was performed in steam atmosphere and the clad sample did not present any significant mark of oxidation. Nevertheless, CEA proposed to fulfil its analysis on the basis of other experimental results.

Risk of clad fracture at quenching
When the critical flux is reached during the transients, there is a large clad temperature increase. Afterwards, there is a phase of clad re-wetting. This quenching phase could induce a fracture of the clad. CEA said that the cladding material is restored at high temperatures and resists to such quenches. Indeed, quenches beginning at 1100°C are often used in manufacturing processes and does not lead to significant deformation.

3.2 Strain limit

The value of 3.65% retained by CEA for the strain limit is issued from several dynamic tensile tests performed on clad rings at several temperatures (20°C to 1100°C) and having provided values for the total elongation. These tests gave also yield strength and tensile strength values. The strain rate was about 100%.s^{-1} (i.e 1% for 10 ms) and was representative of the phenomena kinetics occurring during fast reactivity insertion transients. The strain limit of 3.65% is one half of the minimum value of the rupture elongation measured during all the tests. IRSN raised the following questions in concern with the choice of the strain limit:

Choice of the strain limit as a function of the rupture elongation
IRSN said that the choice of a rupture criterion based on the total elongation is valid for secondary loads. During the transient, the strain is imposed during the PCMI phase but not after the pellet-to-clad gap re-opening. For this latter case, CEA answered that the load is an imposed pressure. However, because of the clad strain, the pressure decreases with time. It was further showed that this loading situation is less severe than an imposed strain. IRSN agreed and considered that loads resulting from the 'imposed strain' type are the enveloping situation for the clad loads during the transient thus justifying the use of the total strain as a limit.

Bi-axiality of the stresses
IRSN examined the representativeness of the tests made on the clad rings with regard to the bi-axiality of the stresses as this point can modify the value of the rupture elongation. During the PCMI phase, the ratio between the two components of the clad deformation (ε_z and ε_θ) is positive while this ratio is negative for the tests made on the clad rings. This effect is important for rods with a high burn-up for which clad and fuel pellets are " stuck " or when the cladding material is a zirconium alloy which anisotropy may lead to a large reduction of the rupture elongation [1]. As the CABRI core rods have a very low burn-up (about 100 MWd/t) and are made of stainless steel having an isotropic behaviour, IRSN considers that the factor 2 used to assess the clad strain limit is sufficient to account for the effects of bi-axiality.

Risks of damage related to cyclic loadings
IRSN considered that the damage related to cyclic loadings was not considered. Afterwards CEA provided a study coupling the primary loads (in relation with internal rod pressure) and the secondary loads (in relation with the thermal gradient in the clad thickness) for several cycles (for CABRI, one cycle corresponds to one fast transient). These load combinations were studied by Bree [2] who provided a diagram defining a zone where the couple primary loads-secondary loads does not lead to excessive strains. For CABRI, when the number of cycles increases, the couple primary-loads secondary-loads tends towards an asymptotic value that lies within the non failure zone of the Bree diagram.

4. Examination of the methodology proposed to compute the fuel rods thermo-mechanical behaviour

The SCANAIR computer code [3] is devoted to the modelling of the complex physical phenomena occurring during fast power transients. Three modules are closely linked:
-   The thermal module calculates the radial conduction in the fuel and the clad, as well as clad-to-coolant heat transfer in sodium or water conditions. The coolant flow is computed thanks to a one-dimension single-phase fluid model.
-   The fission gas behaviour module calculates the swelling of fission gas bubbles, the grain boundary failure within the fuel and the gas flow into free volumes.
-   The mechanical module calculates the strain contributions to the fuel and clad deformation (thermal expansion, elastic, plastic, strain simulating the fuel expansion induced by the presence of cracks and fuel swelling due to gaseous fission product).

The fuel and clad thermo-mechanical models were qualified using separate effects tests and integral tests performed in CABRI-REP-Na programme. A specific validation of the clad-to-water heat transfer has been done for conditions representative of the CABRI core fuel rods

(flow rate, pressure and temperature). This validation is based on the comparison to experimental results of tests performed in NSRR reactor and PATRICIA CEA facility for fast transient transfers. The validation is also demonstrated for late phase film boiling by comparison to WINFRITH test results.

In the SCANAIR code, the clad-to-coolant heat transfer is described by a classical heat transfer coefficient approach which is estimated by correlations. The water boiling phenomena (that increase the heat transfer in nucleate boiling and degrade it in transition boiling) and film boiling are modelled. Heat transfer correlations are often semi or completely empirical and are validated in steady state conditions. During fast transient conditions, the radial temperature profile in the coolant can be much steeper than in steady state conditions and the shape of the boiling curve is different (see Figure 1).
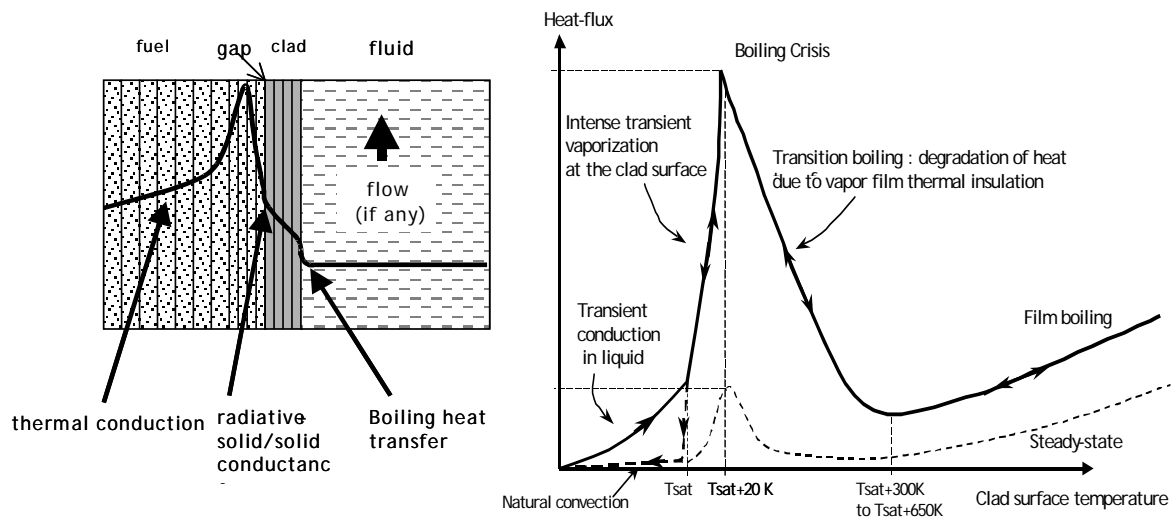

Fig 1: Clad-to-water heat transfer modelling in SCANAIR

The maximal temperature reached during fast transient is mainly linked to the boiling crisis occurrence and the film boiling coefficient. Thus a specific critical heat flux correlation has been developed for transient conditions, leading to higher critical heat flux compared to steady condition. A specific film boiling coefficient based on the Sakurai model [4] and derived from the Bromley correlation has also been implemented. In NSRR tests, in the early stage of the film boiling regime (i.e. when the clad temperature reaches its maximum value), the experimental heat fluxes recorded are 3 to 5 times higher than the predicted values [5]. Therefore a correcting coefficient has been applied on the Sakurai correlation.
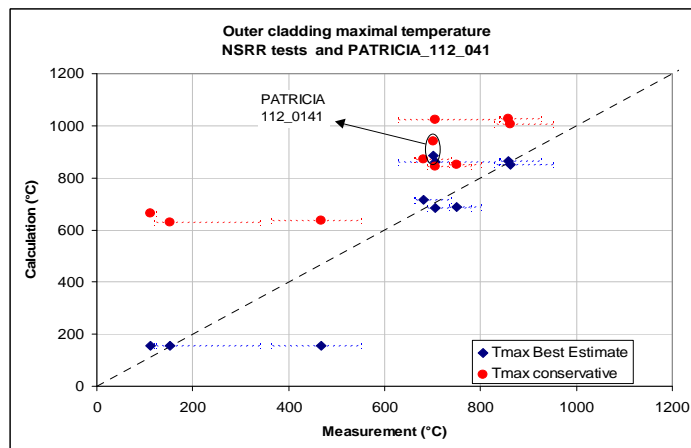

Fig2 : Comparison of computed and measured maximal outer cladding temperature reached during NSRR and PATRICIA 112_041 tests

The comparison between clad temperature measurements and calculations in NSRR and PATRICIA tests shows that the calculation generally overestimates the measured temperatures (see Figure 2). Finally two kinds of calculations have been performed: one with the best-estimated SCANAIR parameters and one with conservative parameters to get conservative results for safety analysis.

5. Comparison of the new criteria to integral experiments

CEA analysis focused on the clad failure modes (steel melting and ductile rupture). However integral experiments realized in SPERT reactor and NSRR reactor used to define failure criteria based on energy deposited in rod during the transient. The rods used during these tests had mechanical characteristics close to those of the rods of the CABRI reactor (UO$_2$ fuel and stainless steel clad). The energy deposition leading to rod failure is in the range of 240 cal/g.

IRSN thus completed his assessment to check the coherence between the results of the SPERT-CDC tests [6, 7, 8] and NSRR tests [9] and the criteria proposed by the CEA. In practice, IRSN calculated by means of the SCANAIR code the maximal energy which would be deposited in a rod, during a power insertion test, leading to reach of the criteria proposed by CEA. For the most severe transients, IRSN's study showed that the allowable clad temperature (1300°C) is reached for 236 cal/g and the strain limit for 287 cal/g. These results show that the limiting parameter is the clad temperature as seen during the tests. Also, the demonstration made by CEA is consistent with the energy deposition limit.

6. Conclusion

CEA has completed its safety demonstration including the additional items identified by IRSN, who concludes that the new criteria and the associated safety demonstration give now an acceptable guarantee against rod failure during fast transients. Nevertheless, IRSN claims and maintains that it is necessary to inspect several driver core fuel rods after some fast transients in order to check the absence of damage of the clad.

7. References

[1] Metallurgical transactions Vol.16A – 1985. - "*Influence of multiaxial states of stress of the hydrogen embrittlement of Zirconium alloy sheet*" - F. YUNCHANG, D.A KOSS

[2] Journal of strain analysis – Vol. 12 N°3 – pp 226-238 1967 – "*Elastic Plastic behaviour of thin tubes subjected to internal pressure and intermittent high heat fluxes with application to fast nuclear reactor fuel elements*" – J. Bree

[3] Proc of IAEA TCM on Fuel Behavior Under Transient and LOCA Conditions, Halden, Norway, September 10-14, 2001 - "*The SCANAIR Code Version 3.2: Main features and Status of Qualification*" - E. Federici, F. Lamare, V. Bessiron, J. Papin

[4] Nucl. Eng. Des., 120[2–3], 271–280 (1990) - "*Correlations for sub-cooled pool film boiling heat transfer from large surfaces with different configurations*" - A. Sakurai, M. Shiotsu, K. Hata

[5] J. Nucl. Sci. Tech, Vol. 44 [5] (2007) - "*Clad-to-coolant heat transfer in NSRR experiments*" - V. Bessiron, T. Sugiyama, T. Fuketa

[6] Report NUREG/CR-0269 August 1978 - "*Light water reactor fuel response during reactivity initiated accident experiments*" - T. Fujishiro, P. E. Macdonald, R.L. Johnson, R.K. MacCardell

[7] Report IDO-ITR-100 October 1968 – "*Transient irradiation of ¾ inch od stainless steel clad oxide fuel rods to 570 cal/g UO2*" - J.A McClure, L. J. Siefken

[8] Report IDO-ITR-101 November 1968 – "*Transient irradiation of 0.466-inch od stainless steel clad oxide fuel rods to 300 cal/g UO2*" - L.A. Stephan C.S. Olsen

[9] Journal of Nuclear Science and Technology 23(12), pp 1051~1063 December 1986 – "*Failure Behaviour of Stainless Steel Clad Fuel Rod under Simulated Reactivity Initiated Accident Condition*" - S. Shiozawa, S. Saito

VALIDATION OF PLTEMP/ANL V3.6 CODE FOR EVALUATION OF SAFETY MARGINS AT THE BR2 REACTOR

RERTR Program, Nuclear Engineering Division
Argonne National Laboratory
Argonne, Illinois 60439, USA

S.KALCHEVA[1], A.P.OLSON[2], E.KOONEN[1] AND J.E.MATOS[2]

[1]SCK•CEN, BR2 Reactor Department
Boeretang, 2400 Mol – Belgium
[2]RERTR Program, Nuclear Engineering Division, Argonne National Laboratory,
Cass Avenue, IL 60439 Argonne – USA

VALIDATION OF PLTEMP/ANL V3.6 CODE FOR EVALUATION OF SAFETY MARGINS AT THE BR2 REACTOR

S.KALCHEVA[1], A.P.OLSON[2],
E.KOONEN[1] AND J.E.MATOS[2]

[1]SCK•CEN, BR2 Reactor Department
Boeretang, 2400 Mol – Belgium
[2]RERTR Program, Nuclear Engineering Division, Argonne National Laboratory,
Cass Avenue, IL 60439 Argonne – USA

ABSTRACT

The aim in this paper is to validate the PLTEMP/ANL V3.6 code for thermal hydraulics analysis of the BR2 reactor at steady-state operation under forced flow cooling conditions. Hot channel factors and operation limiting conditions based on selected safety system settings (SSS) with uncertainties were reviewed and included into PLTEMP. Safety margins to ONB (Onset-of-Nucleate-Boiling) and to FI (Flow Instability) are calculated for the BR2 HEU fuelled core and compared with the existing safety limits for the heat fluxes in SAR-BR2. A preliminary thermal-hydraulics analysis is performed for the LEU (UMo) fuel preserving the geometrical parameters of the standard BR2 fuel assembly. Power peaking factors evaluated by MCNP for both HEU and LEU fuel assemblies are included in PLTEMP. Thermal-hydraulics studies are extended to include conditions of natural circulation cooling. The margins to ONB and to FI are estimated for both HEU and LEU cores.

1.   Introduction

This paper presents a thermal hydraulics analysis at steady state operational conditions, which is a mandatory part of the safety studies needed for the conversion of the reactor BR2 from HEU to LEU. The safety margins at the BR2 reactor have been determined in 70's using the code of S. Fabrega [1]. The purpose in this paper is to review and to repeat the major part of the studies in order to validate PLTEMP/ANL code [2] for the thermal hydraulics calculations of the BR2 reactor. The geometrical BR2 standard, six-tube fuel assembly model has been developed at Argonne National Laboratory. As a first step, hot channel factors and operating limiting conditions (power, inlet mass flow, inlet pressure and temperature) based on selected safety system settings with uncertainties were reviewed and included into PLTEMP. The safety margins to ONB (Onset-of-Nucleate-Boiling) and to FI (Flow Instability) are calculated for the BR2 HEU fuelled core under forced flow conditions. A preliminary feasibility study with U-Mo dispersion fuels has shown that the current fuel assembly design would not change in the conversion of the BR2 reactor from HEU to LEU fuel. Therefore, a preliminary thermal-hydraulics analysis has been performed by PLTEMP for the LEU fuel preserving the geometrical parameters of the standard BR2 fuel assembly. Power peaking factors evaluated by MCNP for both HEU and LEU fuel assemblies are included in PLTEMP. Thermal-hydraulics studies are extended to include conditions of natural circulation cooling.

2.   Review of thermal-hydraulics studies for the BR2 reactor [3-4]
2.1   Determination of maximum heat flux at nominal operating conditions

The maximum heat flux at nominal operating conditions is calculated from the power generated in the hottest fuel channel with the implementation of Hot Spot Factors (HSF) according with the following formulae:

$$q_{max}^{nom} = \frac{P_i}{SK} \cdot R_i \cdot f_i \cdot K_{th} \qquad (1)$$

$$q_{max\,H2O} = K \cdot K_{th} \cdot q_{max}^{nom} = \frac{P_i}{S} \cdot R_i \cdot f_i \qquad (2)$$

Where: P_i [W] is the power generated in the fuel cell 'i'; S [cm^2] is the total heated surface of the fuel element; K=1.055 is coefficient taking into account the fraction of the total power that is generated in the coolant channels; K_{th}=1 to 0.945 is correction diffusion coefficient taking into account the non-uniform heat distribution over the plate thickness; R_i=1.52 to 1.38 is axial peaking factor; f_i=1.48 to 1.3 is azimuth peaking factor.

2.2 Determination of fabrication tolerances and thermal-hydraulic uncertainties

The errors affecting the maximum value of the heat flux include: (i) the errors of the neutronic measurements in determination of the fuel power per channel and the errors in axial and azimuth power peaking factors; (ii) the manufacturing tolerances in the fuel density and in the quantity of burnable absorber in the fuel elements. The following uncertainties have been determined: error in determination of the specific power of a fresh fuel element: $\varepsilon_1 = 18.7\%$; error in determination of the axial peaking factor, $\varepsilon_2 = 7\%$; error in determination of the azimuth peaking factor, $\varepsilon_3 = 7\%$; uncertainties of the surface of the fuel meat, $\varepsilon_4 = 4\%$; error in the correction coefficient K, $\varepsilon_5 = 1\%$; uncertainties in determination of the fuel concentration in the fuel plates, $\varepsilon_6 = 20\%$.

To establish an operational limit, in addition to the errors and tolerances, a correction factor is considered for the effective power deposited in the coolant flow and for the thermal diffusion of heat through the fuel cladding. Assuming a statistical distribution of all errors, influencing the calculated heat flux, the following 'security factors' have been determined: (i) 'security factor' for the maximum probable heat flux at the hot spot: this flux has to be compared to the heat flux giving an allowed wall temperature of fuel cladding, which corresponds to the nominal hydraulic conditions:

$$s_{q\,max}^{hot\,spot} = 1 + \sqrt{\sum_{i=1}^{5} \varepsilon_i^2} = 1.22 \qquad (3)$$

(ii) 'security factor' for the maximum probable mean heat flux along the hot streamline: from the point of view of flow instability, taking into account the total void fraction in the water gap, this flux has to be compared with the heat flux giving a possible flow instability at the nominal hydraulic conditions, where all factors and tolerances are taken with the most unfavourable value:

$$s_{q\,max}^{hot\,line} = 1 + \sqrt{\sum_{i=1}^{6} \varepsilon_i^2} = 1.30 \qquad (4)$$

2.3 Determination of maximum admissible heat flux

The Onset of Nucleate Boiling (ONB) (Bergles & Rohsenow) with sub-cooling occurs when the fuel temperature exceeds the saturation temperature of the coolant by ΔT_{onb}. The model of Hsu, calculated by Bergles and Rohsenow for maximum heat flux 600 W/cm^2 at nominal hydraulics conditions, gave $\Delta T_{onb} = 9.5^0 C$ using the following expression:

$$\Delta T_{ONB}[^\circ C] = 0.555 \left\{ \frac{q[W/cm^2]}{0.1053p^{1.156}[bar]} \right\}^{\frac{p^{0.0234}}{2.17}} \tag{5}$$

The Fully Developed Nucleate Boiling (FNB) is given by the formula of Forster & Greif. For the temperature, corresponding to maximum heat flux 600 W/cm² at nominal hydraulics conditions, was obtained: $\Delta T_{FNB} = 24^0 C$, calculated by the following formula:

$$\Delta T_{FNB}[^\circ C] = 4.57q^{0.35}[W/cm^2]p^{-0.23} \quad \text{for } 1 < p < 12 \text{ bar} \tag{6}$$

The occurrence of vapour is determined by an equation for the equilibrium of the effective forces on the surface of the growing bubble, which is adjacent to the wall channel. At conditions of strongly sub-cooling and low pressure in the middle of the bubble, the occurrence of local boiling is marked by loss of pressure due to friction. The code of S.Fabrega [1] uses a critical factor for calculating the friction coefficient under sub-cooled boiling, ξ, which comes from experimental results of R.Ricque & S.Siboul and M.Courtaud & K.Schleisiek for two-phase flow studies in rectangular sections:

$$\xi = \frac{T_{single\ phase}^{plate} - T_{sat} - \Delta T_{FNB}}{T_{single\ phase}^{plate} - T_{fluid} - \Delta T_{FNB}} \tag{7}$$

By using the code of S.Fabrega at the BR2 reactor, this factor becomes ξ ~ 0.50 when the pressure drop on a fuel plate is minimum, near the flow instability.

The maximum admissible heat flux is determined by combining the most unfavourable uncertainties: minimum water gap (-10%), D=0.27 cm; loss of pressure at the inlet, equal to 0.06 MPa for pressure drop on the fuel plates 0.21 MPa; loss of pressure due to friction, by ~ 10%; admissible reduction of superheat, ΔT_{FNB}, ~ 15%; heat transfer coefficient, reduction by 15%; taking into account the uncertainties of the thermal-hydraulics correlations, the loss of pressure by friction and acceleration at boiling will be overestimated by 25%; the error in the determination of the water speed in the coolant channel is about 10% (between 10.4 and 9.5 m/s). The maximum probable temperature at the hot spot is determined by the following formula:

$$T_{max\ probable} = T_{max\ probable}^{coolant} + \frac{q_{max\ probable}}{h_{min}} \tag{8}$$

2.4   List of constants used by the code of S.Fabrega [1]

The formula of Forster and Greif is used for the superheat temperature at ONB:

$$\Delta T_{ONB}[^\circ C] = 4.57q^{0.35}[W/cm^2]p^{-0.23}[bar] \tag{9}$$

The formula of Sieder-Tate is used for the Nusselt number to simple phase:

$$Nu = \frac{h}{\rho cv} = 0.023Re^{-0.20}Pr^{-2/3}\left(\frac{\mu}{\mu_{plate}}\right)^{0.14} \tag{10}$$

The formula of Darcy is used for the loss of pressure due to friction:

$$\frac{\partial F}{\partial z} = \frac{\Lambda}{D} \rho \frac{v^2}{2} \qquad (11)$$

Where: Λ - Darcy's number; μ - dynamic viscosity; v – coolant velocity; ρ - specific mass; D – hydraulic diameter; Pr – Prandtl number; Re – Reynolds number. For turbulent flow and a coarse wall, $\Lambda_0 \sim a.Re^{-b}$ ($Re < 49800, a = 0.316; b = 0.25; Re > 49800, a = 0,184; b = 0,2$).

For hot wall: $\Lambda = \Lambda_0 \left(\dfrac{\mu}{\mu_{plate}} \right)^c , c = 0.182 + \dfrac{8000}{Re + 18000}$.

The following 'security coefficients' (i.e., hot spot factors) are used by the code of S. Fabrega: for superheat at boiling, local FNB: 15%; for heat transfer coefficient: 15%; for loss of initial pressure: 0.06 ata; for loss of pressure due to friction: 10%; for loss of pressure at local boiling: 25%; the tolerance of the water gap is 10%; for the possible heat flux: 30%.

2.5 Results of the code of S.Fabrega

The calculation results for the maximum heat flux and flow limits in the BR2 reactor are summarized in Table I. The calculations are performed for the configuration 7B-MFBS, channel B0, loaded with fresh fuel element of type 6nG at the following reference initial conditions: PRCA 4 -1302 = 1.20 MPa (inlet pressure); DPRCA 4 -1301 = 0.30 MPa ($v_{coolant}$ = 10.4 m/s cold; $\Delta P_{fuel\ plates}$=0.21 MPa); TRCA 4-1301 = 40^0 C (inlet temperature).

Table I. Maximum heat flux and flow limits for HEU fuelled BR2 core, calculated by the TH code of S.Fabrega [3-4].

V [m/s]	ΔP [MPa]	Q_{max} [W/cm^2] (normal FI)	Q_{max} [W/cm^2] (FNB-probable)	Q_{max} [W/cm^2] (ONB-probable)
11	2.323	1396.1	705.2	626.7
10.4	2.100	1336.5	675.6	603.2
10	1.957	1296.1	655.7	585.2
9	1.619	1190.1	605.0	538.4
8	1.310	1078.9	548.5	490.5
7	1.030	963.3	490.4	441.3
6	0.780	841.0	430.8	389.8
5	0.564	718.1	369.1	334.4
4	0.382	594.0	305.2	278.2
3	0.231	459.5	238.9	219.3
2	0.114	311.3	169.3	157.1

3. Review of Hot Channel Factors (HCF)

In this Chapter we review the uncertainties of the neutronic measurements at the BR2 reactor and manufacturing tolerances of the fuel elements in order to determine the Hot Channel Factors, which have been introduced into the PLTEMP code. The Hot Channel Factors for HEU (93% U5) fuelled core, which are used in the calculations presented in this paper, are given in Table II. The same HCF are used to determine the power and flow limits in the LEU-fuelled core (U-8Mo, 7.5 g/cc, cadmium wires, D=0.5 mm).

Table II. Hot Channel Factors for BR2 standard HEU fuel (93% U5), which are used in the calculations by PLTEMP.

Uncertainty	Type of tolerance	Effect on bulk ΔT, fraction	value	Tolerance, fraction	Hot Channel factors				
					Heat flux, Fq	Channel flow rate, Fw	Heat transf. coeff., Fh	Chan. Temp. rise, Fbulk	Film temp. rise, Ffilm
Al cladding, [mm]	random		0.381 to 0.304	0.25	1.25				1.25
U5 homog.				0.20	1.20				1.20
U5 loading per plate				0.00	1.00			1.00	1.00
Power density		0.5		0.20	1.20			1.10	1.20
Water gap, [mm]	random	1.00	3.00 to 2.7	0.11		1.20	1.04	1.20	1.04
Flow distr. (water speed, m/s)		1.00	10.4 to 9.5	0.10		1.10	1.07	1.10	1.07
Random errors combined					**1.38**	**1.22**	**1.08**	**1.25**	**1.39**
Power measur.	systematic			0.06	1.06			1.06	1.06
Flow measurem.				0.02		1.02	1.00	1.02	1.00
Heat transfer coef.				0.15			1.15		1.15
Systematic errors combined					**1.06**	**1.02**	**1.15**	**1.08**	**1.22**
Product of random and systematic errors					1.46	1.24	1.24	1.35	1.70

4. Implementation of PLTEMP/ANL V3.6 [2] for the thermal-hydraulics calculations of BR2

PLTEMP/ANL V3.6 is a FORTRAN program that obtains a steady-state flow and temperature solution for a nuclear reactor core, or for a single fuel assembly. It is based on an evolutionary sequence of "PLTEMP" codes in use at ANL for the past 20 years. Fuelled and non-fuelled regions are modeled. Each fuel assembly consists of one or more plates or tubes separated by coolant channels. The temperature solution is effectively 2-dimensional. It begins with a one-dimensional solution across the fuel plates/tubes within a given fuel assembly, at the entrance to the assembly. The temperature solution is repeated for each axial node along the length of the coolant channel. The geometry may be either slab or radial, corresponding to fuel assemblies made from a series of flat (or slightly curved) plates, or from nested tubes. A variety of thermal-hydraulic correlations are available with which to determine safety margins such as Onset-of- Nucleate boiling (ONB), departure from nucleate boiling (DNB), and onset of flow instability (FI). Coolant properties for either light or heavy water are obtained from FORTRAN functions rather than from tables. The code is intended for thermal-hydraulic analysis of research reactor performance in the sub-cooled boiling regime. Both turbulent and laminar flow regimes can be modeled. Options to calculate both forced flow and natural circulation are available.

A PLTEMP solution is accomplished in three steps. The first step is a nominal or best-estimate calculations with all HCF equal to 1.0. A best-estimate calculation employs only nominal values in the evaluation of the fuel plate surface temperature, while the limiting calculation, executed during the second and the third step of PLTEMP run, includes the effects of manufacturing tolerances and operational and modelling uncertainties. The second step is a repeat of the nominal calculation with the reactor power increased and the reactor flow and heat transfer coefficient reduced in order to take into account the uncertainties in power and flow measurements, and the uncertainty of the Nusselt number correlations. The third step applies the HCF to all the bulk coolant and film temperature rises and the clad surface heat fluxes obtained in the second step.

5. Calculation results

The aim of this study is to determine using PLTEMP code [2] the power, heat flux and flow limits in the BR2 core loaded with HEU standard BR2 fuel (93% U5) and to compare with the safety limits, which have been established in 70's by the code of S. Fabrega [1], [3]. For this purpose, the same initial conditions as in the calculations of 70's (see beginning of Sect. 2.5) have been introduced into PLTEMP.

The power and flow limits presented in this chapter are compared for different choices of the single phase heat correlation, including those of Sieder-Tate, Dittus-Boelter, Colburn, Petukhov & Popov and another Russian correlation. For the detection of the Onset of Nucleate Boiling, used for ONB thermal margin, the calculations are performed and compared for the correlations of Bergles & Rohsenow and Forster & Greif. For the treatment of the Hot Channel Factors (HCF) the correlation of Labuntsov has been chosen, although the comparison with the other HCF - options (e.g., the correlations of Mirshak-Durant-Towell, Mishima, Weatherhead, Groeneveld 1995 lookup table) has given equivalent result for the power and flow limits at a given single phase heat transfer correlation selector. The onset of excursive – flow instability is based on the correlation of Whittle & Forgan.

5.1. Power and flow limits in BR2, HEU-fuelled core

In this section we present calculations for the power, heat flux and flow limits for the **HEU – core**. The power peaking factors for the UAlx fuel, 93% enriched U5 with 1.3 g/cc uranium density and burnable absorbers B_4C and Sm_2O_3, homogeneously mixed with the fuel in the fuel meat have been calculated by MCNP (see Fig. 1). The initial average fuel power of the fuel assembly is equal to 2.58 MW, assuming that the total reactor power is equal to 55 MW, distributed over 32 fuel assemblies loaded in the core channels. For the thermal conductivity of the aluminium cladding we use 150 W/m-K° and 80 W/m-K° for the fuel meat [4]. The power and flow diagrams, determining the regimes at nominal operation are given in Fig. 2 and Fig. 3. Comparison between the limiting values obtained by PLTEMP with those of FABREGA (see Table I) is shown at Fig. 3. As can be seen from Fig. 3, at nominal initial operation conditions the results of FABREGA are close to the results obtained by PLTEMP for the single phase heat transfer correlation of Sieder-Tate [3-4]. This is in accordance with the information given in the documentation about SAR-BR2, which has been discussed in Sect. 2.4 of this paper. The dependence of the maximum outer fuel-to-clad surface temperature, T_{onb} vs. the maximum heat flux is demonstrated in Fig. 4.

5.2. Power and flow limits in BR2, UMO-fuelled core

In this section we present calculations for the power, heat flux and flow limits in the **LEU – core.** The power peaking factors for the U-8Mo fuel, 20% U5 enrichment fuel, 7.5 g/cc uranium density and with cadmium wires of diameter D=0.5 mm are given in Fig. 1. The initial average fuel power of the fuel assembly is equal to 2.75 MW, at the same total reactor power of 55 MW as in the HEU core, distributed over 32 fuel assemblies loaded in the core channels. For the thermal conductivity of the cladding we use 180 W/m-K° and 14 W/m-K°

for the U-8Mo fuel meat [5]. The power and flow diagrams, determining the regimes at nominal operation in the LEU – core are given in Fig. 5 and Fig. 6. In Fig. 7 we compare the power, heat flux and flow limits for the both HEU and LEU cores.
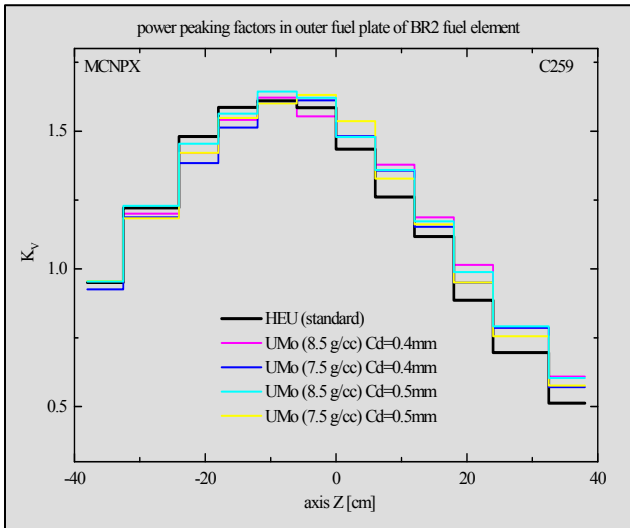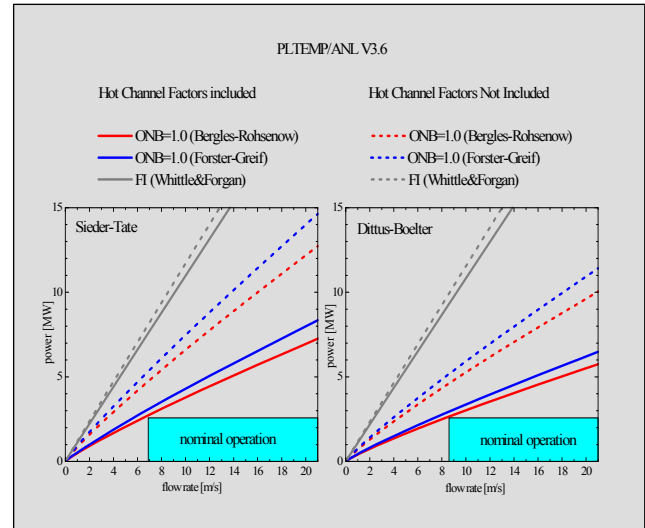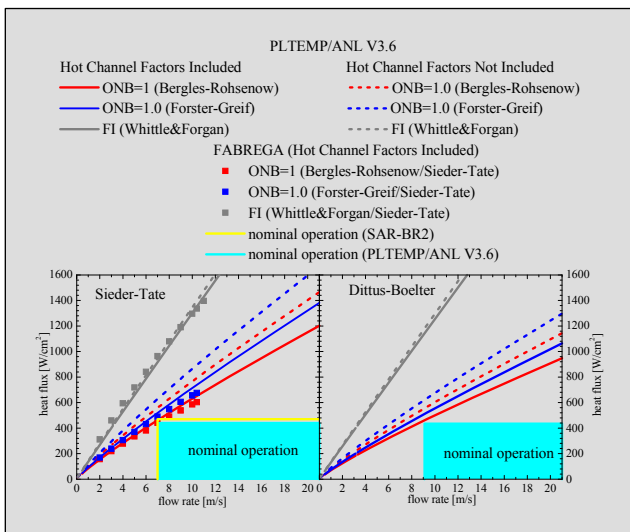

Fig. 1.

Fig. 2.

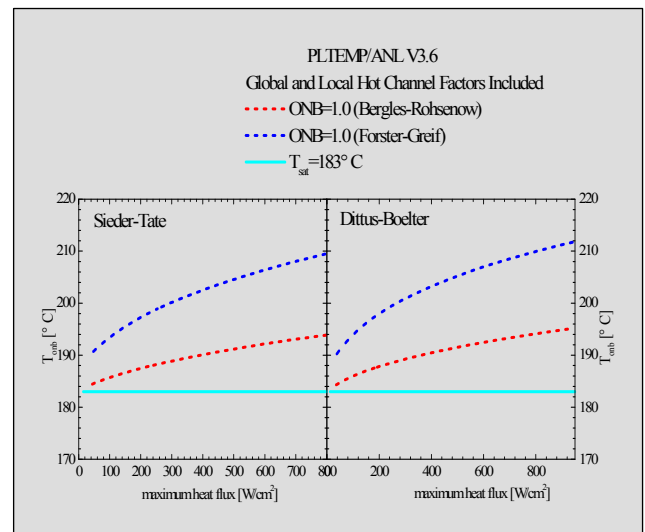Fig. 3.

Fig. 4.

Figure 1. Power peaking factors in the fuel plates of a standard BR2 fuel element calculated with MCNP.
Figure 2. Power and flow limits in HEU – fuelled core, calculated by PLTEMP.
Figure 3. Heat flux and flow limits in HEU – fuelled core, calculated by PLTEMP.
Figure 4. Fuel-to-clad interface outer temperature vs. maximum heat flux in HEU – fuelled core, calculated by PLTEMP.
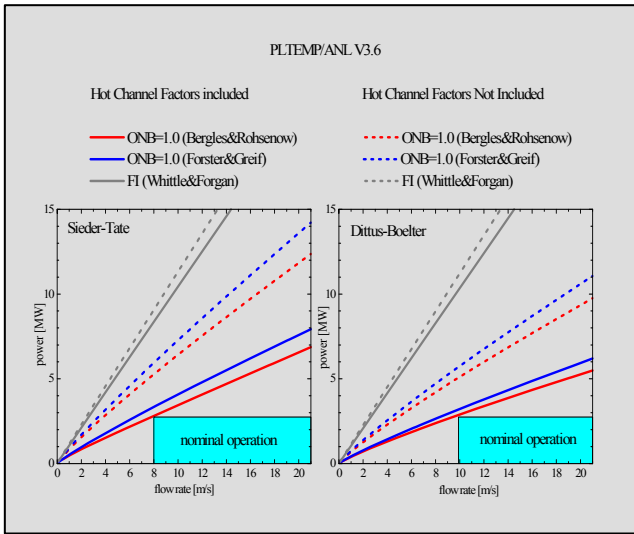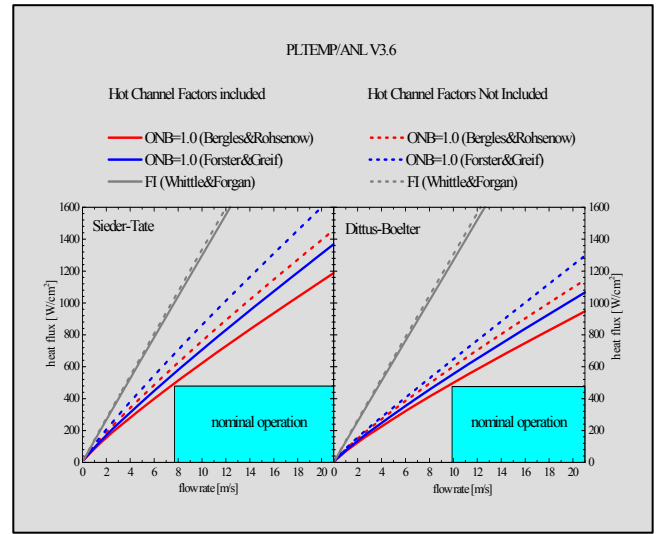
Fig. 5.

Fig. 6.
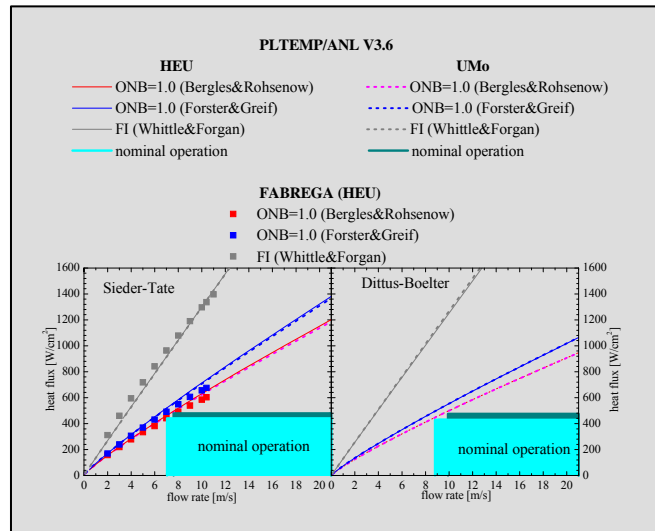
Fig. 7.

Figure 5. Power and flow limits in UMo – fuelled core, calculated by PLTEMP.
Figure 6. Heat flux and flow limits in UMo – fuelled core, calculated by PLTEMP.
Figure 7. Comparison of heat flux and flow limits for HEU and UMo – cores at forced flow operation conditions.

6. Conclusions

Detailed thermal-hydraulics analyses have been performed by PLTEMP/ANL V3.6 code for the BR2, HEU and LEU fuelled cores at steady-state operation under the conditions of forced flow cooling. The following results were obtained at nominal initial operation conditions, with included HCF and actual coolant flow of 10.4 m/s.

For **HEU core:**
- the *maximum output power* to ONB (Bergles & Rohsenow) is equal to 4.0 MW and to 4.5 MW (Forster & Greif) for the single phase heat transfer correlation of Sieder-Tate and to 3.2 MW (B. & R.) and to 3.6 MW (F. & G.) for the single phase heat transfer

correlation of Dittus-Boelter; the power level at which FI (Whittle & Forgan) could occur is equal to 11.4 MW for the single phase heat transfer correlation of Sieder-Tate and to 11.3 MW for the single phase heat transfer correlation of Dittus-Boelter;

- the *maximum heat flux* to ONB (Bergles & Rohsenow) is equal to 667 W/cm^2 and to 753 W/cm^2 (Forster & Greif) for the single phase heat transfer correlation of Sieder-Tate and to 528 W/cm^2 (B. & R.) and to 585 W/cm^2 (F. & G.) for the single phase heat transfer correlation of Dittus-Boelter; the maximum heat flux at which FI (Whittle & Forgan) could occur is equal to 1353 W/cm^2 for the single phase heat transfer correlation of Sieder-Tate and to 1302 W/cm^2 for the single phase heat transfer correlation of Dittus-Boelter;
- the results for the heat flux limits obtained by the code FABREGA are as follows: the maximum heat flux to ONB (Bergles & Rohsenow) is equal to 603 W/cm^2; 676 W/cm^2 (Forster & Greif) and 1336 W/cm^2 at FI (all values are obtained for the single phase heat transfer correlation of Sieder-Tate).

For **LEU core:**
- the *maximum output power* to ONB (Bergles & Rohsenow) is equal to 3.8 MW and to 4.3 MW (Forster & Greif) for the single phase heat transfer correlation of Sieder-Tate and to 3.1 MW (B. & R.) and to 3.4 MW (F. & G.) for the single phase heat transfer correlation of Dittus-Boelter; the power level at which FI (Whittle & Forgan) could occur is equal to 10.9 MW for the single phase heat transfer correlation of Sieder-Tate and 10.8 MW for the single phase heat transfer correlation of Dittus-Boelter;
- the *maximum heat flux* to ONB (Bergles & Rohsenow) is equal to 657 W/cm^2 and to 744 W/cm^2 (Forster & Greif) for the single phase heat transfer correlation of Sieder-Tate and to 528 W/cm^2 (B. & R.) and to 585 W/cm^2 (Forster & Greif) for the single phase heat transfer correlation of Dittus-Boelter; the maximum heat flux at which FI (Whittle & Forgan) could occur is equal to 1350 W/cm^2 for the single phase heat transfer correlation of Sieder-Tate and to 1317 W/cm^2 for the single phase heat transfer correlation of Dittus-Boelter;

The comparison of the obtained by PLTEMP power and flow limits for the HEU fuelled core with those of FABREGA, has shown that the results of FABREGA are close (lower by ~ 8 %) to a PLTEMP solution for single phase heat transfer correlation of Sieder-Tate. For the temperature limit of the cladding, T_{onb}, was obtained that it exceeds the saturation temperature of the coolant (T_{sat}=183° C) by ΔT_{onb} ~ 9.5° C (for Bergles & Rohsenow correlation) and by ΔT_{onb} ~ 25° C (for Forster & Greif correlation). These values confirm the obtained in the 70's temperature limits for the cladding of HEU with the code of S.Fabrega. The main results for the power and flow limits at nominal operation conditions (P_{in}=1.20 MPa, $\Delta P_{fuel\ plates}$=0.21 MPa; T_{in}=40° C; V=10.4 m/s) with included HCF are summarized in Tables III and IV. The results of the thermal-hydraulics analyses by PLTEMP/ANL V3.6 have shown that the power and flow limits in the LEU-UMo fuelled core would increase by about 8% in comparison to the HEU core for the same total BR2 reactor power, P_{BR2}=55 MW.

The margins to ONB and to FI have been also determined at conditions of natural circulation flow. The following results were obtained:

For **HEU core** *without-with* included HCF: the *maximum output power* to ONB (Bergles & Rohsenow) is equal to 83 kW-48 kW and to 86 kW-50 kW (Forster & Greif); the power level at which FI (Whittle & Forgan) could occur is equal to 422 kW-383 kW.

For **LEU core** *without-with* included HCF: the *maximum output power* to ONB (Bergles & Rohsenow) is equal to 84 kW-49 kW and to 87 kW-51 kW (Forster & Greif); the power level at which FI (Whittle & Forgan) could occur is equal to 423 kW-386 kW.

Table III. Maximum heat flux [W/cm^2] / maximum output power [MW] in BR2 core at nominal operation conditions. In brackets is given $\Delta T_{onb}=T_{clad}-T_{sat}$ (where: T_{clad} is the maximum outer clad surface temperature; $T_{sat}=183°C$).

Single phase heat correlation option	Correlations for margins to ONB and to FI	HEU		UMo
		FABREGA	PLTEMP	PLTEMP
Sieder-Tate	Bergles & Rohsenow	603 (9.4°C)	666.7 / 4.00 (10.2°C)	657.1 / 3.78 (10.0°C)
	Forster & Greif	675.6 (24 °C)	752.6 / 4.52 (26.8°C)	744.2 / 4.29 (25.6°C)
	Whittle & Forgan	1336.5	1353.4 / 11.42	1349.9 / 10.86
Dittus-Boelter	Bergles & Rohsenow	–	528.1 / 3.20 (9.1°C)	527.7 / 3.06 (9.2°C)
	Forster & Greif	–	585.3 / 3.56 (24.5°C)	585.2 / 3.40 (24.6°C)
	Whittle & Forgan	–	1302.3 / 11.26	1316.6 / 10.76

Table IV. Maximum heat flux [W/cm^2]/maximum T_{clad} [°C]/minimum flow rate [m/s]/ minimum ONB ratio at nominal operating conditions for $P_{BR2}=55$ MW. $Q_{max}(HEU)=470$ W/cm^2 (SAR-BR2, experimental tests).

Single phase heat correlation option	Correlations to ONB	HEU ($P_{FE}=2.58$ MW)	UMo ($P_{FE}=2.75W$)
		PLTEMP	PLTEMP
Sieder-Tate	Bergles & Rohsenow	440.0/147.2/7.0/1.42	478.9/155.4/7.6/1.30
	Forster & Greif	440.0/147.2/7.0/1.57	478.9/155.4/7.6/1.44
Dittus-Boelter	Bergles & Rohsenow	435.4/166.8/9.1/1.20	475.4/177.8/9.9/1.10
	Forster & Greif	435.4/166.8/9.1/1.32	475.4/177.8/9.9/1.21

7. References

[1] S. Fabrega, "Le calcule thermique des réacteurs de recherché refroidis a l'eau" – CEA-R-4114 (1971).

[2] A. P. Olson and M. Kalimullah, "Users Guide to the PLTEMP/ANL V3.6 code", November 3, 2008, RERTR Program, Argonne National Laboratory.

[3] A. Beeckmans, H. Lenders, F. Leonard, "Definition du flux de chaleur maximum admissible dans les conditionnes normales de refroidissement d'une charge du réacteur BR2", CEN-Euroatom, Dépit. BR2, 72.0616 (1977).

[4] E. Koonen, F. Joppen, A. Beeckmans et al. SAR001-BR2, Volume 2: BR2 operation and operational safety. March 2002.

[5] U -Mo Fuels Handbook. Version 1.0. Compiled by J. Rest, Y. S. Kim, G. L. Hofman ANL and M.K. Meyer and S. L. Hayes, INL. RERTR-ANL, June 2006.

ROLE OF
RELAP/SCDAPSIM IN RESEARCH REACTOR SAFETY

C. M. ALLISON, J. K. HOHORST,
Innovative Systems Software, LLC
Idaho Falls, Idaho 83404 USA
iss@relap.com
A. J. D'ARCY
South African Nuclear Energy Corporation (NECSA)
Pretoria, South Africa
alan@necsa.co.za

ABSTRACT

The RELAP/SCDAPSIM code, designed to predict the behaviour of reactor systems during normal and accident conditions, is being developed as part of the international SCDAP Development and Training Program (SDTP). SDTP consists of more than 60 organizations in 28 countries supporting the development of technology, software, and training materials for the nuclear industry. The program members and licensed software users include universities, research organizations, regulatory organizations, vendors, and utilities located in Europe, Asia, Latin America, Africa, and the United States. Innovative Systems Software (ISS) is the administrator for the program. RELAP/SCDAPSIM is used by program members and licensed users to support a variety of activities. The paper provides a brief review of the applications of the code to the simulation and analysis of research reactors in the United States, Europe, Asia, and Africa. An example showing the application of the code to the SAFARI-1 research reactor in South Africa for licensing analysis and for use in an operator training simulator (SAFSIM) is included in the paper.

1.0 Introduction

The RELAP/SCDAPSIM code, designed to predict the behaviour of reactor systems during normal and accident conditions, is being developed as part of the international SCDAP Development and Training Program (SDTP) [1,2]. SDTP consists of nearly 60 organizations in 28 countries supporting the development of technology, software, and training materials for the nuclear industry. The program members and licensed software users include universities, research organizations, regulatory organizations, vendors, and utilities located in Europe, Asia, Latin America, Africa, and the United States. Innovative Systems Software (ISS) is the administrator for the program.

Three main versions of RELAP/SCDAPSIM, as described in Section 2, are currently used by program members and licensed users to support a variety of activities. RELAP/SCDAPSIM/MOD3.2 and MOD3.4 are production versions of the code and are used by licensed and program members for critical applications such as research reactor and nuclear power plant applications. The most advanced production version, MOD3.4, is also used for general user training and for the design and analysis of severe accident related experiments such as those performed in the Phebus and Quench facilities. In turn, these experiments are used to improve the detailed fuel behaviour and other severe accident-related models in MOD3.4 and MOD4.0. MOD4.0 is currently available only to program members and is used primarily to develop advanced modelling options and to support graduate research programs and training. Section 3 highlights various research reactor

1

applications. An example showing the application of the code to the SAFARI-1 research reactor in South Africa for licensing analysis and for use in an operator training simulator (SAFSIM) is included.

2.0 RELAP/SCDAPSIM

RELAP/SCDAPSIM uses the publicly available RELAP/MOD3.3[3] and SCDAP/RELAP5/MOD3.2[4] models developed by the US Nuclear Regulatory Commission in combination with proprietary (a) advanced programming and numerical methods, (b) user options, and (c) models developed by ISS and other members of the SDTP. These enhancements allow the code to run faster and more reliably than the original US NRC codes. MOD3.4 and MOD4.0 can also run a much wider variety of transients including low pressure transients with the presence of non-condensable gases such as those occurring during mid-loop operations in LWRs, in pool type reactors, or in spent fuel storage facilities.

The most advanced version of the code, RELAP/SCDAPSIM/MOD4.0[5], is the first version of RELAP or SCDAP/RELAP5 completely rewritten to FORTRAN 90/95/2000 standards. This is a significant benefit for the program members that are using the code for the development of advanced models and user options such as the coupling of the code to other analysis packages. Coupled 3D reactor kinetics and coupled RELAP/SCDAPSIM-SAMPSON [6] calculations are examples where MOD4.0 is used because of a significant reduction in the code development effort and expense to link the packages. MOD4.0 also includes advanced numerical options such as improved time advancement algorithms, improved water property tables, and improved model coding. As a result the code can reliably run complex multi-dimensional problems faster than real time on inexpensive personal computers. Plant simulation and integrated uncertainty analysis are among the most important applications benefiting from the improved speed and reliability of MOD4.0. MOD4.0 includes many enhanced user options to improve the accuracy of the code or to offer new options for the users. For example, the addition of an alternative material property library designed for Zr-Nb cladding materials is important for VVER and CANDU reactor designs, particularly for severe accident related transients. The addition of an advanced water property formulation is important for many transients, in particular those involving super critical water applications.

3.0 RESEARCH REACTOR APPLICATIONS

A combination of RELAP/SCDAPSIM/MOD3.2 and MOD3.4 is being used to analyze research reactors. A brief summary of the early work by several countries was given in Reference [6]. The research reactors noted in this paper include (a) the LVR-15 reactor located at the Nuclear Research Institute in Rez, Czech Republic, (b) the CARR reactor being built in Beijing, China by the China Institute of Atomic Energy, and (c) TRIGA reactors located at the Atomic Energy Research Establishment in Dhaka, Bangladesh and National Nuclear Energy Agency in Bandung Indonesia. LVR-15 is a light-water moderated and cooled pool type reactor with a nominal thermal power of 15 MW. The pool operates at atmospheric pressure with an average coolant temperature in the core of 320 K. The reactor also has closed high pressure/temperature loops suitable for testing of materials under PWR and BWR conditions. The reactor core is composed of several fuel assemblies of Al-U alloy arranged in square concentric tubes. CARR is a tank-in-pool design, cooled and moderated by light water and reflected by heavy water. The rated power is 60 MW. The core consists of plate-type fuel assemblies of Al-U alloy. The Indonesian and Bangladesh TRIGA reactors are pool type reactors with 2 MW and 3 MW thermal power respectively. The reactor cores are composed of solid U-ZrH fuel rods arranged in a hexagonal array and are cooled by water in either forced or natural circulation, depending upon the conditions.

More recently, the analysis of two additional reactor types have been reported in References 7-9. The first is for the SAFARI-1 research reactor located in South Africa [7,8]. The second

2

is the University of Missouri Research Reactor located in the United States [9]. The SAFARI-1 research reactor is a tank-in-pool type reactor operated at a nominal core power of 20MW. The core is cooled and moderated by forced circulation of light water. The reactor core can be operated in a variety of configurations from 24 to 32 fuel assemblies. Figure 1 shows an example of one such configuration. The fuel is U-Si-Al plate-type fuel elements. MURR is a 10 MW pool type reactor design with a pressurized primary coolant loop to cool the fuel region. The pressurized primary system is located in a pool allowing direct heat transfer during normal operation and transition to natural convection under accident conditions. The reflector region, control blade region, and center test hole are cooled by pool water (natural convection).
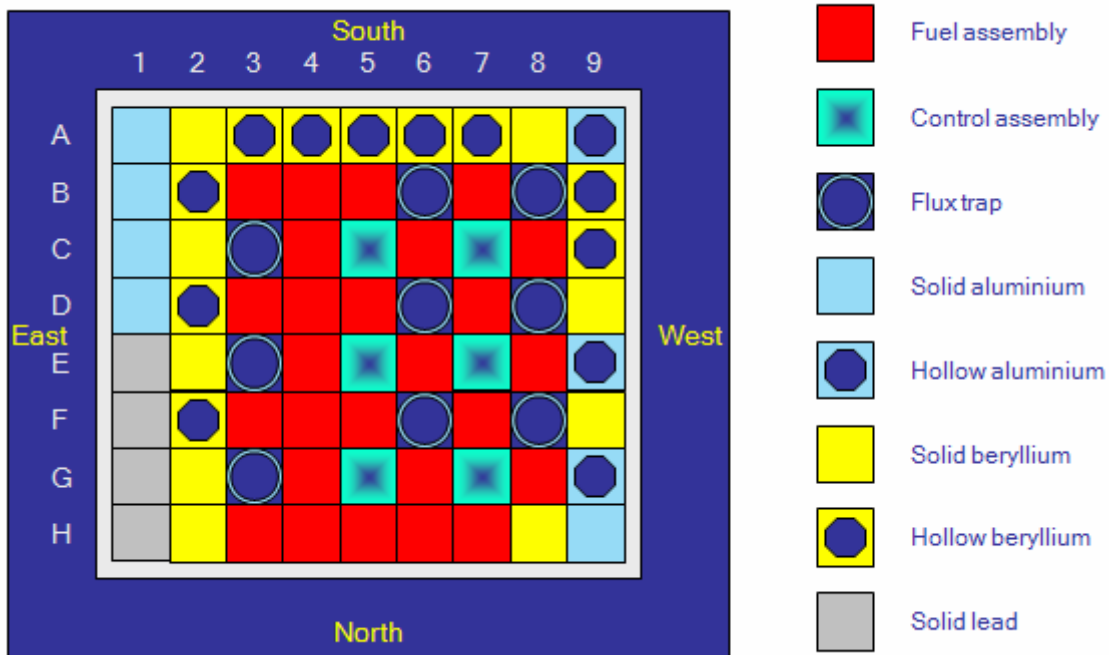

Figure 1: SAFARI-1 Reactor Core Configuration.

Because of the unique reactor designs, the RELAP/SCDAPSIM input models were developed separately by each organization and include a range of different nodalizations as presented in the reference papers. However in general terms, the RELAP/SCDAPSIM input models include all of the major components of each reactor system including the reactor tank, the reactor core and associated structures, and the reactor cooling system including pumps, valves, and heat exchangers. The secondary sides of the heat exchanger(s) are also modelled where appropriate. These input models were qualified through comparison with reactor steady state data, with original vendor safety analysis calculations where available, and with experiments in a limited number of cases.

Figure 2 shows the nodalization used for the SAFARI-1 research reactor. The figure shows the overall system hydrodynamic nodalization with the upper right corner of the figure showing the core nodalization. Note from the insert of the core nodalization diagram that the bypass or unheated channels were modelled separately from the heated fuel assembly channels. The core nodalization also included two separate hot plate channels located on each side of the hottest plate.
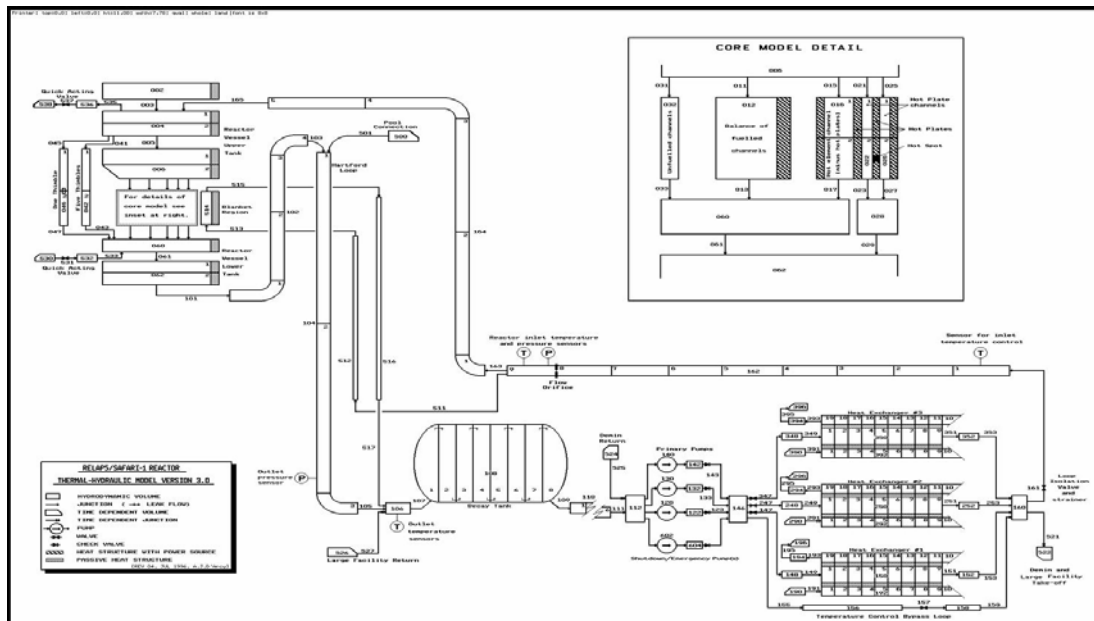
3

Figure 2: RELAP/SCDAPSIM Nodalization of the SAFARI-1 Cooling System.

A wide variety of transients have been analyzed using the code. Examples are included in the references and include reactivity initiated power excursions and loss of flow or coolant transients.

RELAP/SCDAPSIM/MOD3.4 is used as the simulation engine for the SAFSIM PC based training simulator for SAFARI-1. The simulator is used as a training tool for reactor operators. The main purposes of the simulator is to 1) build operator experience, 2) provide operator training at all levels, 3) be a pre-examination for licensed operators, 4) train personnel in the setup of operating modes, 5) develop operating and emergency procedures, 6) analyze operating incidents and occurrences and 7) give the operator a general understanding of reactor behaviour under all sorts of fault and accident conditions. Figure 3 shows the simulator running on a typical PC with dual monitors. Figures 4a and 4b show more detailed pictures of portions of the control panel mimic. As shown by comparison to photographs of the SAFARI-2 control room panel, figures 5a and 5b, the SAFSIM represents the main features of the control room control panel and provides a visually realistic image for training purposes.

At startup SAFSIM displays the reactor control room with the reactor completely shut down and the power supply to the protection mimic switched off. Therefore it is necessary for the trainee to go through the startup of all systems before the reactor can be started. The simulator was designed to give a realistic representation of the reactor and includes a very detailed representation of the reactor's control system using a combination of standard RELAP5 control systems and reactor-specific coded algorithms which are linked to RELAP5 for the simulator. As a result, new operator training or operator retraining, which originally required the actual startup and operation of the reactor, can now be done on the simulator. The simulator also has an instructor's panel from which the instructor can give the operator in training operational problems and challenges during a simulator session. Figure 6 shows the instructor's panel display.
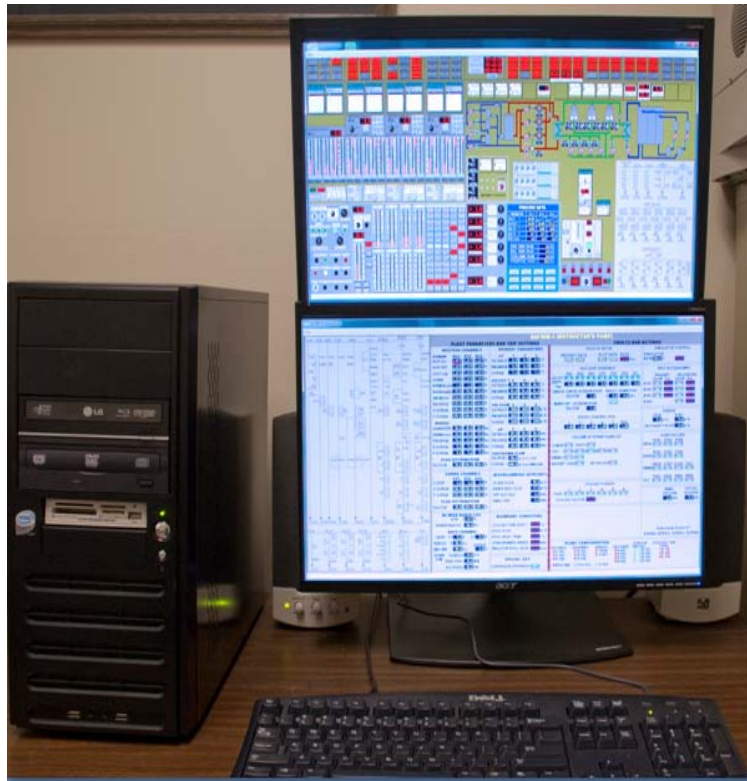
4

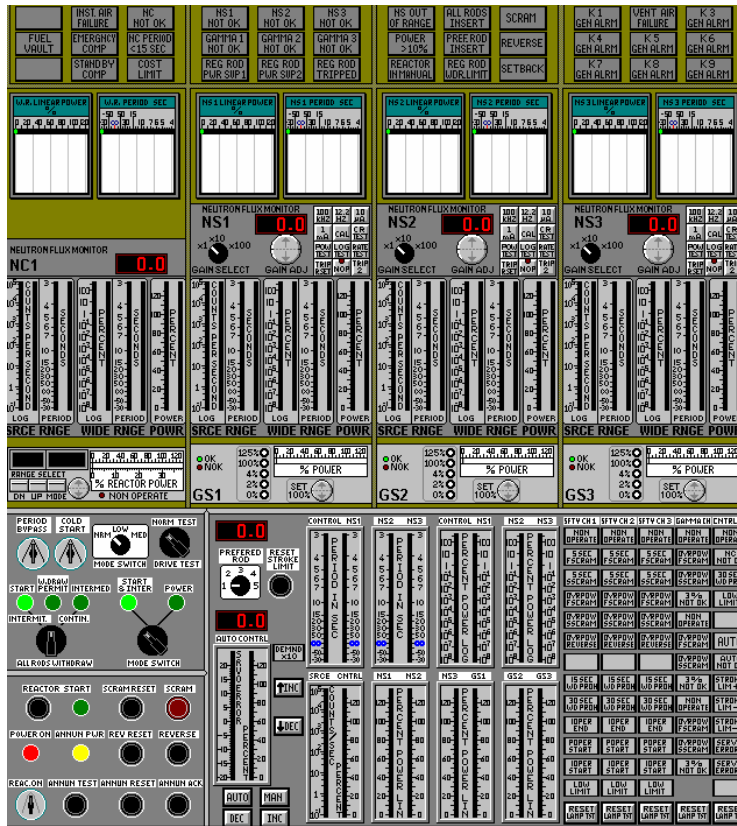Figure 3: SAFSIM running on typical PC with dual monitors.
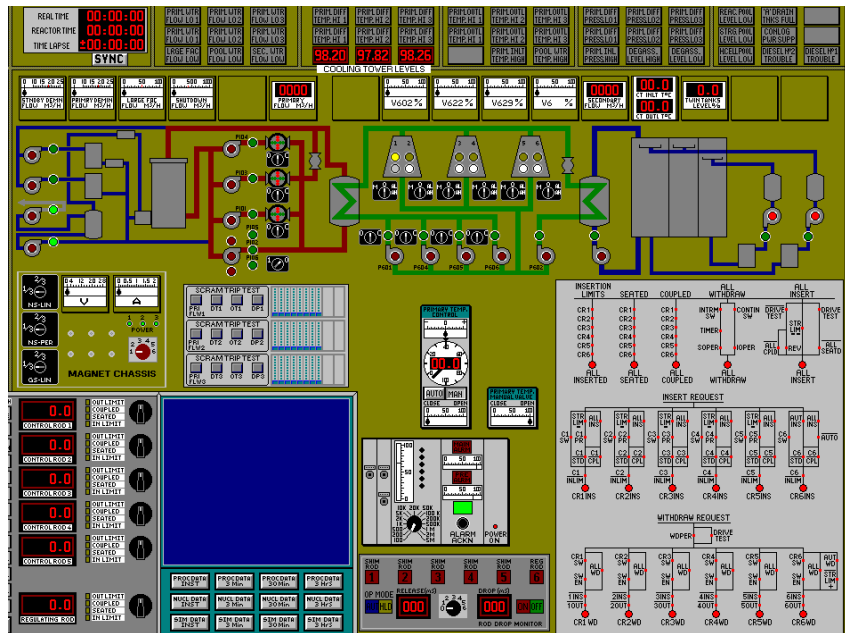

Figure 4a: Control panel mimic.

5

Figure 4b: Control panel mimic.

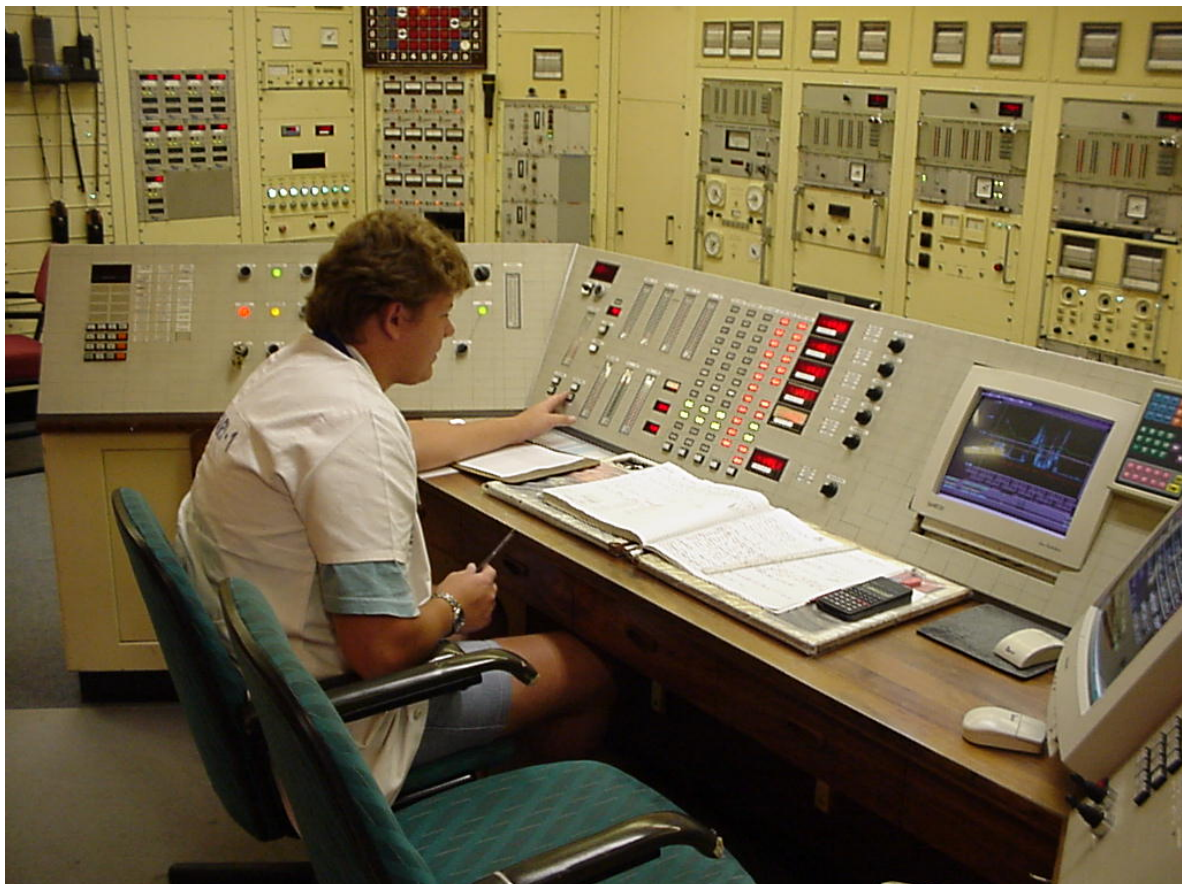Figure 5a: Actual control room panels.

6

Figure 5b: Actual control room panels.

Figure 6: SAFSIM's Instructor's panel display.

7

4.0 References

[1] www.relap.com.

[2] www.sdtp.org.

[3] RELAP5 Code Development Team, "RELAP5/MOD 3.3 Code Manual, Vol 1-8", NUREG/CR-5535/Rev1 (December, 2001).

[4] SCDAP/RELAP5 Development Team, "SCDAP/RELAP5/MOD3.2 Code Manual, Vol. 1-5", NUREG/CR-6150, INEL-96/0422, (July, 1998).

[5] C. M. Allison, R. J. Wagner, L.J.Siefken, J.K. Hohorst, "The Development of RELAP5/SCDAPSIM/MOD4.0 for Reactor System Analysis and Simulation", Proceedings of the 7th International Conference on Nuclear Option in Countries with Small and Medium Electricity Grids, Dubrovnik, Croatia, (May 2008).

[6] A. R. Antariksawan, Md. Q. Huda, T. Liu, J. Zmitkova, C. M. Allison, J. K. Hohorst, "Validation of RELAP/SCDAPSIM/MOD3.4 for Research Reactor Applications", Proceedings of ICONE 13, Beijing, China, (May 2005).

[7] A. Sekhri, A.L. Graham, M. Belal, L.E. Moloko, A.J. D'Arcy, "Thermal hydraulic and safety analyses of a proposed HEU & LEU core for SAFARI-1 research reactor," RRFM Conference, Hamburg, Germany, (2008).

[8] A. Sekhri, A.J. D'Arcy, A.L. Graham, M. Oliver, "Thermal-hydraulic modelling of the SAFARI-1 research reactor using RELAP/SCDAPSIM/MOD3.4" International Conference on the Physics of Reactors, Interlaken, Switzerland, (September, 2008).

[9] R. C. Nelson, J. C. McKibben, K. Kutikkad, L. P. Foyto, "Thermal-Hydraulic Transient Analysis of the Missouri University Research Reactor (MURR)" TRTR Annual Meeting (September, 2007).

8

SEVERE REACTIVITY INJECTION ACCIDENT SIMULATIONS FOR SAFETY ASSESSMENT OF RESEARCH REACTOR

S. PIGNET, C. PELISSOU, R. MEIGNEN

Reactor Safety Division, French Institute for Radiological and Nuclear Safety (IRSN)
B.P. 17, 92262 Fontenay aux Roses Cedex – France

P. LIU, F. GABRIELLI

Institute for Nuclear and Energy Technologies, Forschungszentrum Karlsruhe (FZK),
Hermann-von-Helmholtz-Platz 1, D-76344 Eggenstein-Leopoldshafen – Germany

ABSTRACT

In the frame of safety assessment of research reactor, IRSN studies the consequences of reactivity transient so-called BORAX, more precisely it has appeared necessary to transpose experiments results to new concept of research reactor. For that purpose, the code SIMMER-III, devoted to severe accident simulation, has been adapted and validation work on SPERT experiment has been done in collaboration with FZK/IKET. The results show that SIMMER is accurate to simulate BORAX in a thermal reactor and will be a very convenient tool to transpose experimental results to reactor case. Especially the effects of neutronics feedbacks will be precisely focused on. Furthermore, specific simulations of the steam explosion are computed by a dedicated code developed by IRSN, MC3D. First example of MC3D application to BORAX transient is shown. These two main tools will allow IRSN to deeply analyse the safety demonstration of JHR reactor as far as severe reactivity injection accident is concerned.

1   Introduction

Core disruptive tests carried in the United States in BORAX-I facility in 1954 and in SPERT facility in 1962, as well as the accident which occurred on the 3rd of January 1961 have shown that a control rod withdrawal in a water moderated pool-type reactor with aluminium plates fuel could lead to explosive phenomena. These experiments allowed to understand the phenomenology of the transient ([1], [2]). If the reactivity injection is sufficient, the aluminium of fuel plates starts to melt, whereas the water of the core remains rather cold, then the fuel coolant interaction (FCI) generates the formation of a water steam bubble which expands in the primary circuit with pressure waves. That is why the transient can induce:
- the destruction of a part of the core including experimental devices, which can contain non condensable gas,
- the damage of reactor pool walls,
- the weakening containment lower part,
- a water spray and direct release of fission product in the hall of the reactor,
- a production of hydrogen by the oxidation of aluminium,
- damage of the upper part of containment, due to the increase of pressure in the hall of reactor and eventually an hydrogen deflagration or explosion.

In France, design of research reactor takes into account so-called BORAX transient. For the utility, the purpose is to demonstrate that a BORAX transient can not lead to important radioactive releases in the environment. Until now this demonstration is based on three main assumptions:
- 135 MJ of thermal energy is released in the fuel,
- 100% of the fuel melt,
- 9% of thermal energy is converted in mechanical energy by FCI phenomena;

These values are mainly extracted from the interpretation of BORAX destructive test.

In 2003, IRSN analysed the safety options of a new project of research reactor to be built in South of France: Jules Horowitz Reactor (JHR). At that time it was decided that, because JHR design is quite different from BORAX or SPERT design, it could be useful to develop numerical tool to transpose experimental results to JHR, in order to status on the hypothesis to be taken into account for JHR design [3]. Then IRSN launched a research program with two main goals: the first one consists in analysis of the availability of BORAX result for JHR by means of numerical simulation of the whole transient, and the second deals with the evaluation of consequences of steam explosion on the pool and the hall of the reactor. This research program will allow IRSN to deeply analyse the safety demonstration of JHR reactor which will be supply by the utility.

2   Overview of IRSN research program on BORAX transient

2.1   SIMMER extensions for research reactor modelling

The SIMMER-III multi-physics code system [4] was initially developed for mechanistic safety analyses of liquid metal cooled fast reactors while employing coupled spatial neutron kinetics and thermal hydraulics models. The code is interesting for our study because it couples three physical fields important for BORAX phenomenology, that is to say neutronics, thermohydraulics and structure degradation. In order to analyse the transposition of experimental values from BORAX and SPERT experiments to JHR, efforts are under way at FZK to extend SIMMER application for specific severe accident phenomena in thermal reactors. With this aim the SIMMER neutronics and thermal-hydraulics were extended.

The original set of SIMMER cross-section processing options and the related data libraries was updated [5]. In view of the application to the thermal reactor analyses, 40-group cross-sections libraries (10 groups below 1 eV) were generated by means of the C^4P code and data system [6]. The system includes several fine-group (560 neutron energy groups below 20 MeV) "master" libraries (including f-factors) stored in the Committee of Computer Code Coordination (CCCC) format, which was extended for taking into account properly thermal scattering effects. The fine-group data are based on recent evaluated nuclear data files such as JEF 2.2, JEFF 3.0, JEFF 3.1, JENDL 3.3, ENDF/B-7.

A new technique has been developed and implemented into a test version of the SIMMER code in order to take into account heterogeneity effects in e.g. water cooled systems with pin-type or plate-type fuel, where this effect plays a particularly important role [5], [7]. This technique, potentially applied to fast systems too, is based on employing pre-calculated parameters. These parameters - effective mean chord lengths (for taking into account properly the resonance self-shielding effects) and flux ratios (for taking into account accurately the intra-cell neutron flux distribution in space) - are evaluated by means of a reference cell code [7]. The aim is building tables of parameters representing one or more relevant reactor states to be employed in the neutronics/thermal hydraulics coupled calculations. Further extensions of this technique for transients in which fuel relocation occurs are under development. The extended SIMMER code system was benchmarked against MCNP and ECCO reference codes in a MTR and PWR fuel assembly with respect to criticality and the main reactivity effects (Doppler, moderator temperature and void). Results [5], [7] showed a reasonable agreement among the codes.

Besides modifications and improvements in the neutronics part of the SIMMER-III code, a plate-type fuel pin model [8] has been implemented to the code for well simulating the temperature profile in the plate-type fuels. In order to validate the applicability of the updated SIMMER-III code on the disruptive transient analysis of light water cooled plate-type fuel pin thermal reactors, SPERT I D-12/25 core disruptive tests [2] have been chosen as the benchmark problem. In the SPERT, large reactivity ramp rates were introduced to the reactor core to induce short period of power excursions, among which, three tests conducted with periods of 5.0 msec, 4.6 msec and 3.2 msec resulted in both thermal distortion of the plate and fuel plate melting. All tests performed in the SPERT I D-12/25 facility indicated that the thermal

expansion and steam formation were the effective shutdown mechanisms. In the referred three tests, the inserted reactivity was 2.63$, 2.72$ and 3.55$ respectively.

SIMMER-III simulations on the three disruptive tests have been performed. In order to well model the heat transfer between pin surface and water, coolant channels have been sub-divided into several meshes in the radial direction [8], [9]. The initial near zero-power state was firstly well simulated in order to build up a proper model for the further simulations of the transient tests. As can be seen from Figure 1, comparison between the simulated results and the experimental data indicated that neutron flux profiles in the core have been well represented.
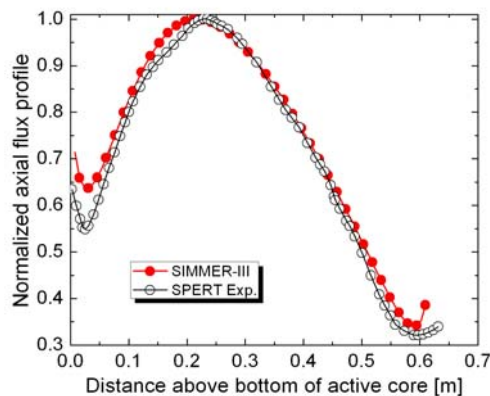
Figure 1: **Normalized axial neutron flux profiles at the initial state**

The three power excursion tests with different periods showed similar transient developing mode. In the tests, reactivity was inserted into the core through the ejection of the transient rods which located in the core center. In SIMMER-III simulations, inserted reactivity was defined directly with a certain ramp rate instead of the modelling of the transient rods' movement. As will be presented in more detail in reference [8], SIMMER-III has well simulated transients of the power, released energy as well as temperatures in all the three cases. Figure 2 shows that SIMMER-III simulated reactor power and released energy agree well with the experimental results in the most disruptive case with a period of 3.2 ms, in which 3.55$ reactivity was inserted. Uncertainties in the modelling are still related to the feedback effects from local boiling and plate expansion.
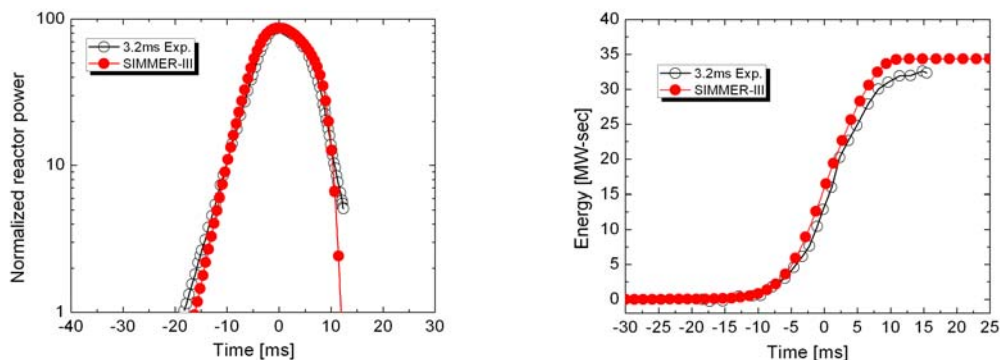
**Figure 2**: **Reactor power and released energy in the case with period of 3.2 ms**

2.2 Modelling of steam explosion with MC3D code

A part from SIMMER III work, the MC3D code is used to evaluate the loads induced by a steam explosion that might follow a BORAX transient. The MC3D code is a modular numerical tool devoted to multidimensional multiphase flow calculations with two main options (named

"applications") for calculating the coarse mixing between the molten fuel and the coolant (premixing) and the consequent explosive interaction [10]. An example of what can be computed with MC3D for analysis of BORAX consequences is described hereafter.

In the present case, the premixing phase has not been computed. It is hypothesized that, as in the SPERT experiment, the transient is so fast that the core is molten without having a noticeable change of geometry. We make then the conservative assumption that the molten plates are equivalent to droplets with a diameter equal to fuel plate width. Due to the high subcooling and rapidity of the transient, the amount of vapour is supposed to be very small (1 %), considering only the existence of a small vapour film along the plate. During the explosion these droplets are transformed into fragments. The size of fragments is taken equal to default value (deduced from experimental data) that is to say 100 microns. The figure 3 shows the propagation of pressure waves in the pool for a case where we do not consider the presence of metallic closed vessel inside the pool. The injected energy is 200 MJ. In the core, and on the floor, the pressure reaches more than 20 MPa. The loads on the wall are limited to about 6 MPa during 7 ms thus leading to an impulse of about 0.05 MPa.s. The fine fragmentation of the core is found to be complete and last for about 3 ms. The duration of the pressure load is related to the height of water above the core and corresponds roughly to the time necessary for the pressure wave to reach the water level and a depressurization wave to propagate downwards. We also find that a large bubble is created, but, due to the constraint given by the important water level, its evolution is limited and its maximum diameter is about 1 m. No real important ejection of water out of the pool is computed.
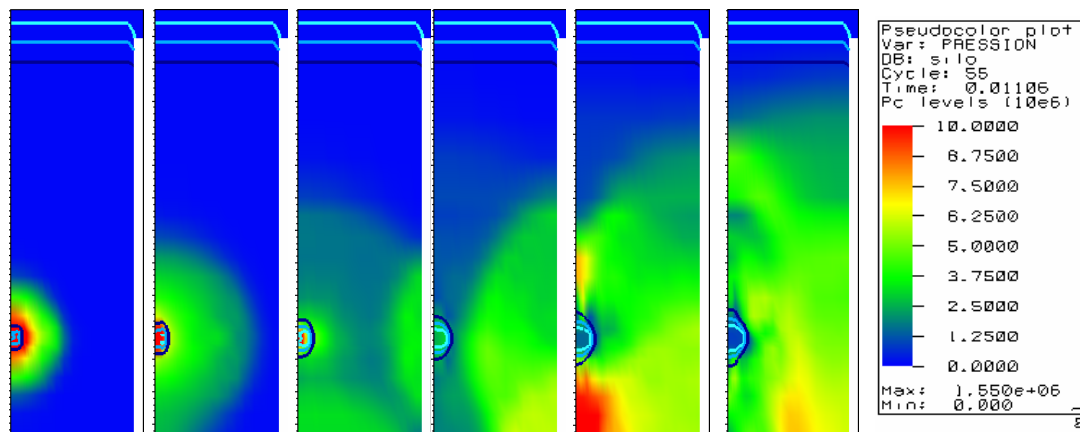
Figure 3 : Evolution of the pressure field during the explosion (Δt = 1 ms, colour scale in MPa). Thick lines are relative to the level of water fraction (30 %(light blue), 50 %, 70 % (dark blue).

This computation does not take into account aluminum oxidation. Though, beyond some threshold temperature, the oxidation in underwater explosions proceeds as fast as the fragmentation itself [11] and strongly affects the energetic of the interaction. Epstein and Fauske [12] explained this phenomenon with the assumption of non-equilibrium in the solidification process of the oxidized phase. Oxidation was observed only with a limited amount in the SPERT experiment. However, the threshold temperature for aluminium is around 1500 K, i.e. for temperatures close to those reached in transients. Currently, MC3D can handle this phenomenon only qualitatively due to the uncertainty regarding the amplitude and kinetics of the oxidation process. Calculations of the ZrEX experiments [13], led us to the conclusion that for the case of zirconium, the characteristic time of oxidation was of the order of some milliseconds, but Epstein and Fauske's modelling leads to consider time scales of the order of 100 µs. Due to the specific geometry involved here, the oxidation can hardly act on the duration of the pressure wave, as explained before. Then oxidation mostly acts on the level of the pressure. As an example, the case with a grade of oxidation of 10 % during the time of interaction (say, first 5 ms), leads to double the pressure load and impulse on the wall. Oxidation during a steam explosion is an important topic of research and an improvement of modelling for a more mechanistic description is planned for next years.

3 Conclusion

Since a few years, IRSN has started an important work around the modelling of severe reactivity injection accident in research reactor. The purpose is to improve the understanding of important parameters and phenomenon to be taken into account for the safety demonstration. This objective leads to adapt, validate and run feasibility studies with the code SIMMER-III. Extensions for SIMMER-III neutronics and thermohydraulics models and validation for SPERT were done in cooperation with FZK. The obtained results show that the code simulates correctly phenomena during the BORAX transient and is now ready to facilitate transposition of experimental results to a reactor case. Next step is then the study of the efficiency of feedbacks in new design of research reactor with low enriched uranium plates. Moreover the work is completed by MC3D computations for estimations of pressure loading on the pool structures. Thanks to these results and in order to evaluate the consequences of BORAX transient, further work is foreseen to study the mechanic behaviour of pool structure during the accident.

4 References

[1] J.R. Dietrich - AECD-3668 report : "*Experimental investigation of the self-limitation of power during reactivity transients in a subcooled, water-moderated reactor*"
[2] R.W. Miller, Alain Sola, R.K. McCardell - IDO16883 report : "*Report of the SPERT- I destructive test program on an aluminium, plate-type, water-moderated reactor*"
[3] G.Biaut, T. Bourgois, G. B. Bruna : -Proc of TOPSAFE 2008 –« Revaluation of BDBA consequences of research reactors »
[4] Tobita, Kondo, Yamano, Morita, Maschek, Coste and Cadiou - Nuclear Technology, 153 [3],245,2006 "*The development of SIMMER-III, an advanced computer program for LMFR safety analysis, and its application to sodium experiments*"
[5] F. Gabrielli, A. Rineiski, W. Maschek, G. Biaut, Proc of PHYSOR 2008, Interlaken, Switzerland, September 14-19, 2008, "*Extension of the SIMMER cross-section processing scheme for safety studies of thermal reactors*"
[6] A. Rineiski, V. Sinitsa, W. Maschek, Proc. of Jahrestagung Kerntechnik, Nuremberg, May 10-12, 2005, "*C^4P, a Multigroup Nuclear CCCC Data Processing System for Reactor Safety and Scenario Studies*"
[7] F. Gabrielli, A. Rineiski, W. Maschek, Proc. of Jahrestagung Kerntechnik, Hamburg, May 27-29, 2005, "*Computation of heterogeneity model parameters for analyses of reactor transients*"
[8] P. Liu, D. Wilhelm, et al., Int. Conf. Mathematics, Computational Methods & Reactor Physics (M&C 2009), Saratoga Springs, New York, May 3-7, 2009, "*Implementation of a Plate-type fuel pin model to a multi-physics code and Benchmark modeling of Special Power Excursion Reactor Tests*"
[9] D. Wilhelm, G. Biaut, Y. Tobita – Nuclear Engineering and Design 238 (2008) 41-48 "*Simmer model of a low enriched uranium non-power reactor*"
[10] R. Meignen - Proceedings of ICAPP '05, Seoul, KOREA, May 15-19, 2005, Paper 5081 "*Status of the Qualification Program of the Multiphase Flow Code MC3D*"
[11] L. Epstein –Nuclear Science and Engineering, 10, 247-253, (1961), "*Correlation and prediction of explosive metal-water reaction temperatures*"
[12] M. Epstein, H.K. Fauske – Nuclear Engineering and Design, 146 (1994), 147-164, "*A cristallization theory of underwater aluminium ignition*"
[13] D.H. CHO, D.R. Armstrong, W.H. Gunther – NUREG/CR-5372, 1998, "*Experiments on interaction between zirconium-containing melt and wate*r".

MCNP Simulation of Permanent Cd-lined Irradiation Channel for Improved Utilization of Commercial MNSR Facilities

S.A. Jonah!, U. Sadiq[2], S. Hankourou[3], Y. A. Ahmed[1]

1 Reactor Engineering Section, Centre for Energy Research and Training, Ahmadu Bello University, Zaria, Nigeria
2 Department of Physics, Ahmadu Bello University, Zaria, Nigeria
3 Department of Physics, Gombe State University, Gombe, Nigeria

Abstract:

The Nigeria MNSR (NIRR-1) is one of the commercial MNSR facilities installed outside China. NIRR-1 was critical in 2004 and has been standardized for routine elemental analysis via the relative NAA method and the k0-INAA technique. In order to eliminate exposure to radiation dose from movable shields and perform activation within a permanently fixed Cd shield, a conceptual permanent Cd lined inside a large outer irradiation of NIRR-1 was simulated using Monte Carlo transport code, MCNP5 version 1.40. Results of neutronics analysis show that the effect of installation of the Cd- liner in the outer irradiation channels on core excess reactivity is less than 0.5 mk and the uniformity of neutron flux in the co-axially arranged irradiation channels is preserved. Data of simulated neutron energy spectrum in the channel with and without the Cd liner are presented.

Furthermore, results of calculated data of Cd-ratios together with advantage factors for the determination of I, Br, C and K in one of the outer irradiation channels of NIRR-1 in geological samples are presented.

Introduction

Miniature Neutron Source Reactors (MNSRs) are compact low-power nuclear research reactors designed and manufactured by the China Institute of Atomic Energy (CIAE), Beijing, China. The seven commercial MNSR and the prototype currently operational in the world are fueled with highly enriched uranium (HEU). Unlike the commercial versions, the prototype MNSR is equipped with a permanent Cd-lined irradiation channel (Hou et al., 1996). The Nigeria MNSR is code-named **Ni**geria **R**esearch **R**eactor**-1** (NIRR-1). NIRR-1 has a tank-in-pool structural configuration and a nominal thermal power rating of 31 kW. With a built-in clean cold core excess reactivity of 3.77 mk measured during the on-site zero-power and criticality experiments, the reactor can operate for a maximum of 4.5 hours at full power (i.e. equivalent to a thermal neutron flux of 1×10^{12} n.cm^{-2}.s^{-1} in the inner irradiation channels). NIRR-1 has been standardized for routine NAA via relative and the k0-standardiation methods (Jonah et al. 2005; 2006; 2009) Like all MNSR facilities, NIRR-1 is specifically designed for use in neutron activation analysis (NAA) but does not have provision for epithermal neutron activation

analysis procedure (ENAA) except via the use of movable thermal neutron shields. In this work, in order to eliminate exposure to radiation dose from movable shields and perform activation within a permanently fixed Cd shield, a conceptual permanent Cd lined inside a large outer irradiation of NIRR-1 was simulated using Monte Carlo transport code, MCNP5 version 1.40. Furthermore, results of calculated data of Cd-ratios together with advantage factors for the determination of I, Br, Cl and K in one of the outer irradiation channels of NIRR-1 in geological samples are presented.

Materials and methods
The Monte Carlo N-Particle (MCNP) code and a set of neutron cross-section data were used to develop an accurate three-dimensional computational model of current NIRR-1 core fueled with HEU (Jonah et al., 2007). The geometry of the reactor core was modeled as closely as possible including the details of all the fuel elements, reactivity regulators, the control rod, all irradiation channels, and Be reflectors. The MCNP code is a general-purpose code for the transport of neutrons, photons and electrons (Breimester, 2000). The neutron energy regime is from 10^{-11} MeV to 20 MeV for all isotopes and up to 150 MeV for some isotopes, the photon energy regime is from 1 keV to 100 GeV, and the electron energy regime is from 1 keV to 1 GeV. The simulation of radiation transport in matter involves the tracking of particles according to established probabilistic laws, commonly known as cross sections. An important feature of the MNCP is capability to calculate k_{eff} eigen values for fissile systems. Like input wase executed as KCODE source problem for criticality calculations using the MCNP5 code version 1.40, which runs on a Linux Cluster in the Computational Reactor Physics laboratory at the Centre for Energy Research and Training, Ahmadu Bello University, Zaria. The Linux Cluster consists of four personal computers, each with 512 MHz processor speed and 1024 M-Byte RAM. It was executed on multiple processors using MPI parallel computing capabilities with MCNP5 executables. All jobs were executed with the "TASK n" option made with 100,000 particles in 400 cycles. One of the basic tally card f4:N, the track length estimate in the cell with different energy bins was constructed for the calculation of axial neutron flux distributions in the irradiation channels according to the 640 group energy structure. An MCNP diagram of NIRR-1 showing a Cd-liner in one of the large outer irradiation channels is depicted in Fig. 1.

According to the Hogdahl convention the Cd-ratio of nuclides of interest can be calculated from the expression given in equation 1.

$$R_{CD} = \frac{f}{Q_o(\alpha)} + 1 \qquad (1)$$

Where,
f is the ratio of thermal-to-epithermal flux ratio determined experimentally,

$Q_o(\alpha)$ is ratio of the resonance integral (I) to the cross section at 2200 m/s corrected for non-ideality of epithermal neutron flux (α)

Details of the conversion of Q_o to $Q_o(\alpha)$ can be found in De Corte and Simonits (2003). ENAA procedure is employed to reduce the influence of interfering elements with high thermal neutron capture cross section in the analysis of elements of interest with high resonance integrals. The enhancement of radionuclide of interest is normally expressed as the advantage factor (AF), which is calculated as the Cd-ratio [$R_{CD}(1)$] of interfering element divided by the Cd-ratio [$R_{CD}(2)$] of element of interest.

$$AF = \frac{R_{CD}(1)}{R_{CD}(2)} \qquad\qquad (2)$$

Results and Discussion

Two input decks were constructed for the current HEU core of NIRR-1 with and without Cd-liner in one of the large outer irradiation channels. The k_{eff} multiplication factors were found to be 1.0042±0.0003 and 1.0047±0.0003 respectively. From these data, it can be shown that the loss of core excess reactivity due to the presence of the Cd-liner in one of the large outer irradiation channel is 0.5 mk. As such, the effect of installation of a Cd-liner in one of the large outer channel on reactor excess reactivity is negligible thus preserving uniformity of the neutron flux in ten irradiation channels of commercial MNSR facilities. Furthermore, data of neutron spectral distribution in 640 group energy structure in the large outer irradiation channel with and without Cd-liner are displayed in Fig. 2. As can be seen in the figure, the neutron spectral distribution in the channel with a Cd-liner is without the thermal neutron energy component with a cut-off energy of approximately 0.5 eV.

In order to further assess the suitability of NIRR-1 for the ENAA procedure, Cd-ratios and the advantage factors were calculated for some elements of interest on the basis of the spectrum parameters of an outer irradiation channel of NIRR-1 and the relevant nuclear data of nuclides of interest taken from De Corte and Simonits, 2003. Results are presented in Table 1 for I, Br, C and K with Na considered as the interfering element. The advantage factors obtained were calculated to be greater than unity for the elements of interest using the outer irradiation channel of NIRR-1 with the following neutron spectrum parameters, f = 48 3±3.3 and α =-0.029±0.003 (Jonah et al. 2005). These values are consistent with experimental data obtained by Stuart et al. 1981 using the SLOWPOKE-2 reactor at Dalhousie University, Halifax, Canada. Since the advatnge factor provides information on the degree to which an element of interest will be enhanced, the provision of Cd-lined irradiation channel will lead to improved utilization of commercial MNSR facilities.

References

Briesmeister, J.F., 2000. MCNP-A general Monte Carlo N-Particle Transport Code Version 4C. LA-13709-M, Los Alamos National Laboratory, USA

De Corte F. and Simonits A. 2003. Recommended nuclear data for use in the k0 standardization of neutron activation analysis. Atomic and Nuclear Data Tables 85, 47 – 67

Hou Xiaolin, Wang Ke, Chai Chifang 1996. Epithermal neutron activation analysis and its application in the Miniature Neutron Source Reactor. J. Radiaonal. Nucl. Chem. 210, 137-148

Jonah, S.A., Balogun, G.I., Umar, I.M., Mayaki, M.C., 2005. Neutron spectrum parameters in irradiation channels of the Nigeria Research Reactor-1 (NIRR-1) for the k_0-NAA standardization. J. Radiaonal. Nucl. Chem. 266, 83-88

Jonah, S.A., Umar, I.M., Oladipo, M.O.A., Adeyemo, D.J., 2006. Standardization of NIRR-1 irradiation and counting facilities for instrumental neutron activation analysis. Appld Rad. & Isotopes, 64, 818-822

Jonah S.A., Liaw J.R., Matos J.E., 2007. Monte Carlo simulation of core physics parameters of the Nigeria Research Reactor-1(NIRR-1)" Annals Nucl. Energy 34, 953-957

Jonah S.A., Sadiq U., Okunade I.O., Funtua I.I. 2009. The use of the k0-IAEA program in NIRR-1 laboratory. . J. Radiaonal. Nucl. Chem. (in press)

Stuart D.C. and Ryan D. 1981. Epithermal neutron activation analysis with a SLOWPOKE nuclear reactor. Canadian Journal of Chemistry 59, 1470 - 1475

Table 1 Nuclear data and calculated RCd and AF of elements of interest by ENAA using an outer irradiation channel of NIRR-1

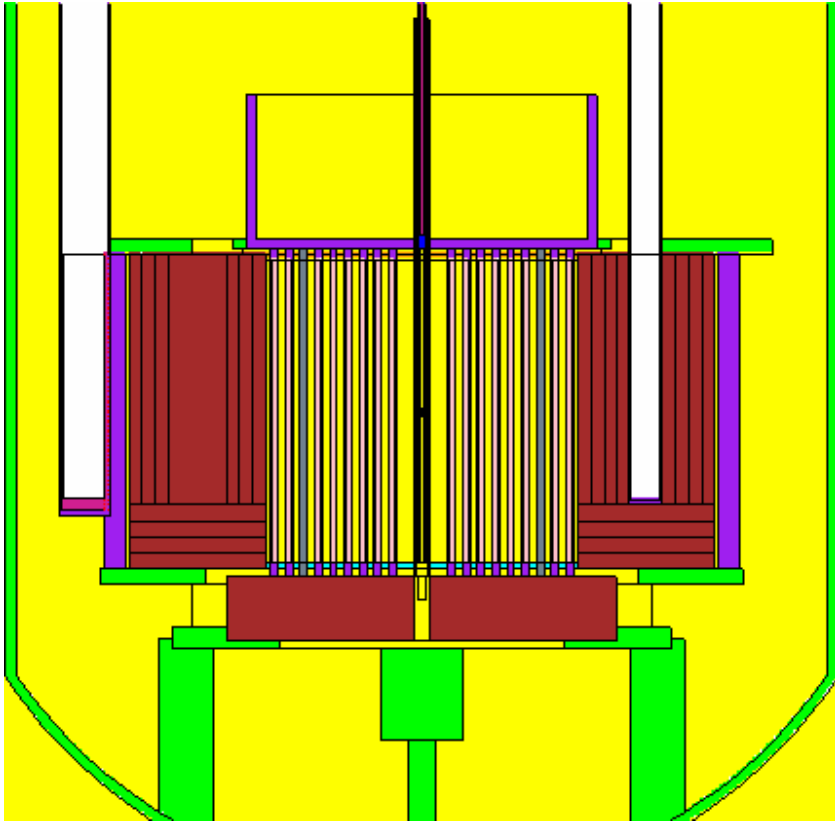| Element	Nuclide	E (keV)	R_{Cd}	AF
I	^{128}I	442.9	2.95	28.1
Br	^{80}Br	616.3	5.04	16.4
Cl	^{38}Cl	1642.7	72.03	1.2
K	^{42}K	1524.6	50.76	1.63
Na	^{24}Na	1368.6	82.86	-

Fig. 1 A geometric diagram of NIRR-1 axial plane from MCNP depicting 0.1 cm Cd liner
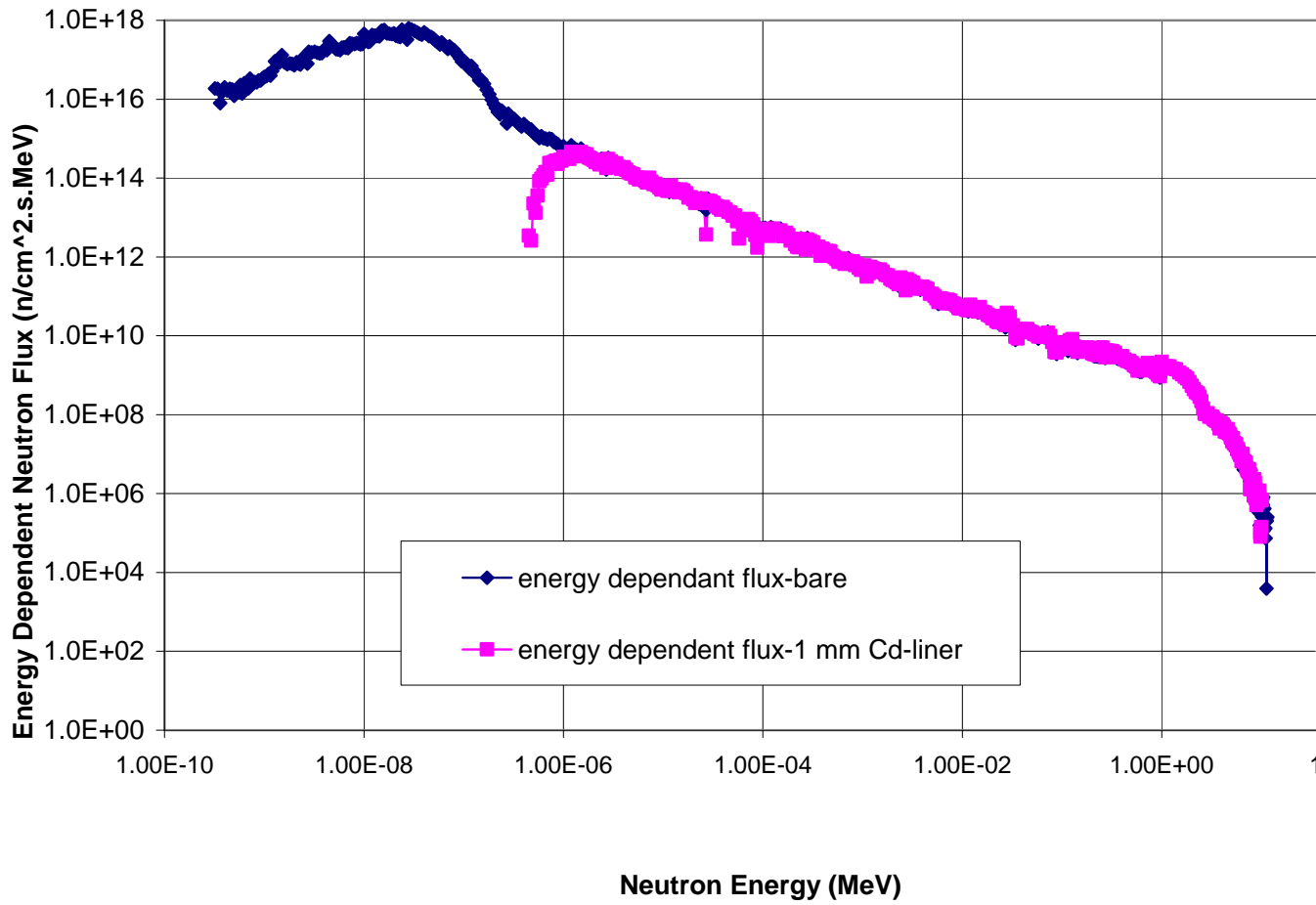in a large outer irradiation channel

Fig. 2 MCNP simulated energy-dependent neutron flux distributions in outer channl of
NIRR-1 with and without Cd-liner

Fuel plate temperatures during operation of FRM II

A. Röhrmoser, W. Petry

Forschungsneutronenquelle Heinz Maier-Leibnitz (FRM II),
Technische Universität München, D-85747 Garching , Germany

ABSTRACT

We present the time averaged temperature distribution of the fuel in the FRM II over a full operations cycle. Because of the single fuel element design the power distribution over the cycle changes clearly as the single control rod moves more and more away from the core center. Any evaluation of the time averaged temperature distribution must take this into account. Therefore the early developed module sequence Mf2dAb that led to the design of the fuel element of FRM II, was used to predict the power density distribution for different time steps of now fully 60 days of full power operation. For any of this time steps there was performed a quasi static temperature evaluation over and through the full fuel plate of FRM II element that is cooled with typical inlet temperature of the primary light water cooling circuit. As a result it can be given the location of the hot temperature maximum, now time averaged and not only for the moment of reactor start (BOC) that was the main point of regard for reactor safety evaluations.

1 Introduction

From the beginning TUM and its working group followed different ways of solutions [1][2] for the development of a high density UMo fuel for reduced enrichment of FRM II. One of our contributions to monolithic fuel was a principal study for FRM II and ended up, besides all the fabrication questions, with the proposition of a thickness gradient of the monolithic UMo foils [3] to avoid too high temperatures. Among others any studies for a new core for FRM II need a careful evaluation of its spatial and timely temperature evolution in the course of the burn-up during operation.

For the FRM II with the actual U_3Si_2 fuel the nominal values of maximum temperature at the cladding surface are given with 98°C for BOL ('begin of life'). Including exactness margins of the calculations a maximum temperature of 119°C at the cladding surface is mentioned in the safety assessment of the FRM II core. With a MEU core the maximum temperatures are expected to tend generally to slightly higher values.

The particular question is now about this aspect of maximum temperatures during operation averaged over a full cycle. Since 2008 this is for FRM II the extended operations cycle of 60 full power days (FPDs). Precicely because it seems that the swelling behavior of the UMo fuel is much more temperature dependant than with the current U_3Si_2 fuel [4] particular attention has to be paid to the temperature evolution during burn-up of the single fuel element.

2 Fuel cycle neutronic calculations for FRM II

TUM developed a very detailed module sequence Mf2dAb, that lead to the single fuel element core design of FRM II till 1990. One of the major aspects during conception phase was the start reactivity but of same interest and indivisible from each other were the topics reactivity loss and power distribution during core burn-up, covering the full reactor cycle. This burn-up procedure shall be depicted here rather shortly.

2.1 Burn-up procedures and flux determination

   a)   The core was therefore partitioned into 7*10 radial/axial burn-up zones

b) There were included the following relevant fission products for build up and burning:
U-234,PU-241,PU-242,ZR-95,NB-95,MO-95,MO-99,MO-100,TC-99,RU-101,RU-102,RU-103, RH-103,RH-105,PD-105,AG-109,J-131,J-135,XE-131,XE-133,CS-133,CS-134,CS-135,CE-141,CE-143,PR-141,PR-143,ND-143,ND-145,ND-147,ND-148,PM-147,PM-148,PM-148m,PM-149,SM-150,SM-151,SM-152,SM-153,EU-153,EU-154,EU-155,EU-156,EU-157,GD-157,ND-146.

c) Other isotopes/actinide chains were added to the library particularly for a FRM compact core:
KR-83,MO-97,CD-113,I-129,LA-139,ZR-93,NP-237,NP-238,NP-239,U-237,PU-238

d) For the more relevant nuclides on the neutron balancing there was provided not only a change of the spectrum with time but also with each radial zone position:

Al-27,Si-28,U-235,U-238 for the fresh fuel plates and
U-236,PU-239,PU-240,XE-235,SM-249 for the more or less direct products

With respect to the general model of flux determination it shall be mentioned that:

o With burn-up the control rod (CR) is drawn out of the core more and more, what changes the flux and power distribution in the core. A vertical 'control rod position search mode' was introduced into the 2D-flux module to find and respect the correct CR position for any time step.

o Inclusion of all beam holes, irradiation positions, secondary sources etc (the user installations UIs) in the heavy water (HW) tank by use of an adapted UI model in the burn-up calculations. The amount of HW was reduced slightly and instead beam tube material introduced, smeared in cylindrical geometry but adapted to different amounts in different radial zones. The overall reactivity loss by the structure material and the HW ousting of the UIs were the two values to fit to in this model; the comparison case were really 3d-calculations with very realistic inclusion of all relevant UIs.

o Besides it were also introduced extra burn-up procedures for a boron ring on bottom of the core and another one for the inner Be block at the end of the CR

As a result there are generated fission power distributions during the fuel cycle. In fact steady state power data are produced for the following time steps:

o 0, 0.5, 3, 10, 20, 30, 40, 48, 52 FPDs and now extended to 60 days of full and enduring operation. The burn-up equations are solved for all the 70 core zones with the flux calculation data of the last time step.

2.2 Control rod driveway in operation

In Picture 1 is shown the CR position as measured during the first 'no-stop'-cycle 6 in 2006 of FRM II compared to the calculated values for 14 time steps of the reactor at operating temperatures.
The agreement to the real operations data, that reach the end point of 52 days, is quite fine over the whole cycle. This means that not only the control rod (CR) position curve is reflected accurately by the DIFF2d flux calculations, but also the burn-up is predicted exactly with inclusion of all the details that are followed by the extensive module sequence MF2dAb. The calculation shows also a maximum cycle length of 60 days at full power with a CR that is then practically fully withdrawn[#].

Another result of these steady state critical calculations for FRM II are the power density distributions in the core for the different time steps. With the module sequence Mf2dAb running now over 60 days of operation, the power density data could be given till the very end of reactor operation. They were used then for the following thermohydraulic calculations.

FRM II operates at totally 20 MW thermal power. Nearly 93% of the thermal power, that is 18.7 MW, are localized between the fuel plates, that is slightly more than. From the remaining 7% of thermal power a small part is localized again in the primary circuit in the central CR region, but most of it outside the primary cooling channel in the heavy water (HW) tank and its installations.

[#] Those extra days of operations reserve are meanwhile confirmed exactly with the first operation of full power duration over 60 days mid of 2008.
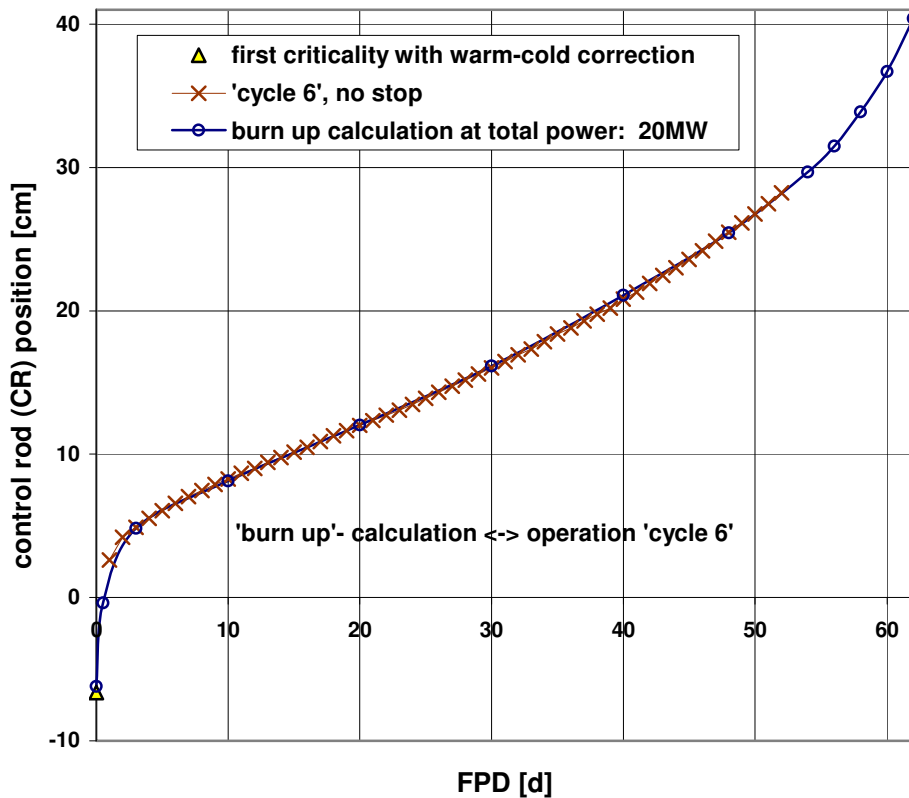
Picture 1:
CR driveway calculated and measured. The red crosses mark the positions given by the first 'no-stop'-operation 'cycle 6' in 2006 of FRM II. The blue dots mark the time steps of the burn-up calculation, that gives in parallel the power distribution data as input for the thermohydraulic temperature evaluation with the code NBK.

3   Detailed temperature evaluation for fuel plates with NBK code

TUM also developed a tailor-made thermohydraulic code NBK [5][6] for the description of all relevant parameters during steady state cooling of the fuel element. It has not been used for safety evaluations where standardized routines are mandatory. However the code NBK includes details that could not be modeled in any of the very few qualified codes that were available at that time. Some of the general features of NBK are:

a)   Full evaluation of the thermohydraulic parameters over the whole length of the cooling channels. That means local coolant speed in the channels for the water; local pressure values, pressure drops; local heat transfer values and resulting temperatures for the water and the wall surfaces.

b)   Evaluation of the thermohydraulics also with differentiation over the width of the cooling channels (the channel edges are also respected). Any 2d-power profile can be regarded.

The very particular features are:

c)   The 2d-power profiles generated at the former neutronic burn-up calculations can be used and are adjusted directly to the 2d-profile of the plates 'meat' layer.

d)   Heat transfer over the width of the plates is evaluated. This is important for the plate sides where the 'meat' layer inside ends abruptly and sees more heat transferring aluminum around; again this is of clear effect for the 'meat' area of FRM II fuel plates, where the uranium density changes abruptly from 3 g/cc to the half value. There are several areas of heat transfer, the two claddings, the 'meat' and the remaining aluminum at the plates sides as well as the edges of the cooling channels which are formed by the inner and outer core tubes. All of them are described by finite elements for the heat transfer.

e)   The involutes shape of the plates and channels is respected. That is, the heat transfer finite element areas in the plates follow the in volute shape and are thus not exactly rectangular. Because of this the plate 'meat layer' sees also different channel areas left and right.

Picture 2:
Original sketch out from [6] to illustrate the tailor-made model of NBK for thermohydraulic calculations between the envolute shaped plates. It is shown a cross section of one cooling channel between two plates at the area of uranium density stepping (3.0 and half value, s. arrow). The cooling channels are divided horizontally each into about 60 threads. Any thread sees a different heating from left and right side. What is not shown here are the finite elements in the cladding and the 'meat' layer which have the same edges as the threads and can transfer heat in both directions of the drawing.
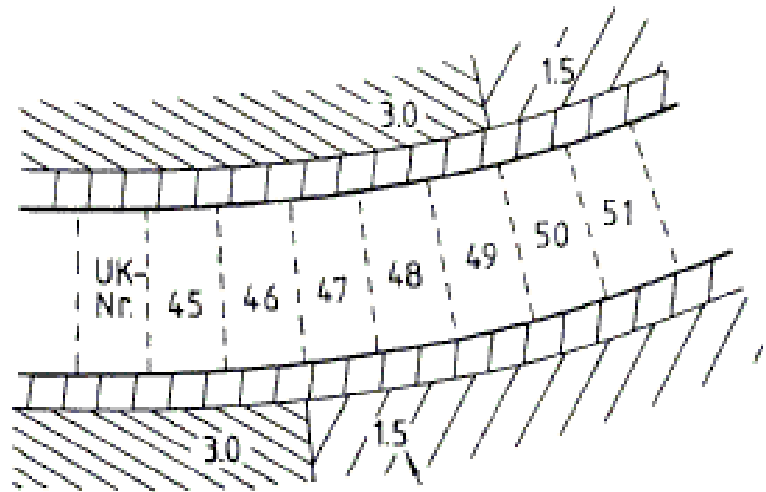
As long as the channel width is kept constant (as done here) there may not be regarded any mass exchange or friction between the channels. The threads are adjusted to the same pressure value at any height.

For the actual work the code was now adapted for:

f) running different states of operation in series. The time steps to be used were now the same as those given by the former neutronic calculations, that simulated now 14 time steps from begin to end of the fully 60 FPDs operation of FRM II.

The temperatures at the surfaces and in the coolant can now be written by the NBK code (together with the calculated channel dimensions) to a specific file and in series for all calculated time steps.

4   Results

Next a program for displaying the data has been adjusted to read the values written by the NBK code and to show the single temperature profiles for any of the time steps as well as an adapted integral, or better averaged value profile. This is shown next.

There where taken rather conservative values for the operation during the calculated cycle. The water inlet temperature was fixed to 38°C. The velocity of the coolant between the plates was taken to be 17.5 m/s in average and the heat transfer coefficient was taken by the formula from Colburn with a wall temperature correction. The formula showed best results in comparable cases [7].
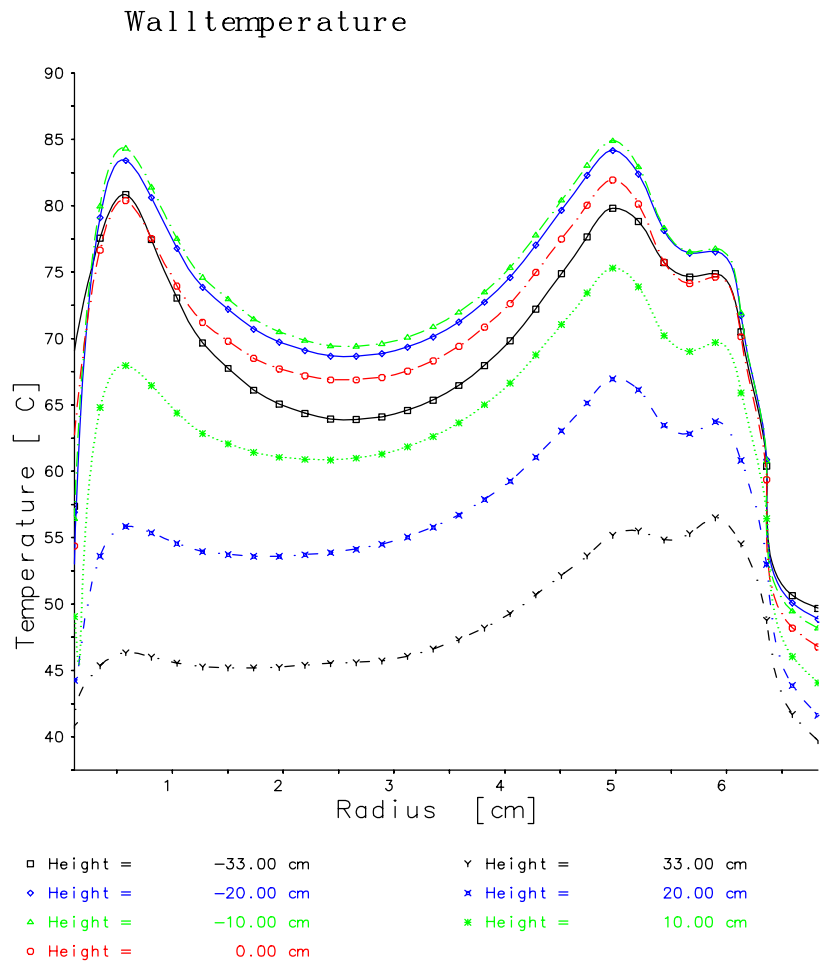
The main result of this work is a more moderate maximum value for the time averaged wall temperature:

• The temperature maxima are fairly smoothened in contrast to the power density with sharp peaks, that are input data here for the thermohydraulic NBK code

• There exist two regions on the plates of practically the same maximum time averaged temperature. Both maximum show up to be rather broad and are located at a height between -5cm and – 20 cm relative to the core center plane. The first maximum is close to the inner side of the channel and the second one more to the channel center slightly inside the edge where the uranium density stepping occurs (about fluid element 45 in Picture 2).

• The time averaged maximum temperatures for FRM II are calculated to be nominally 85°C when taking conservative water inlet temperatures of 38°C.

Fig. 3:
Surface temperature over the width of the typical fuel plate of FRM II averaged over a whole cycle of 60 days of full power operation.
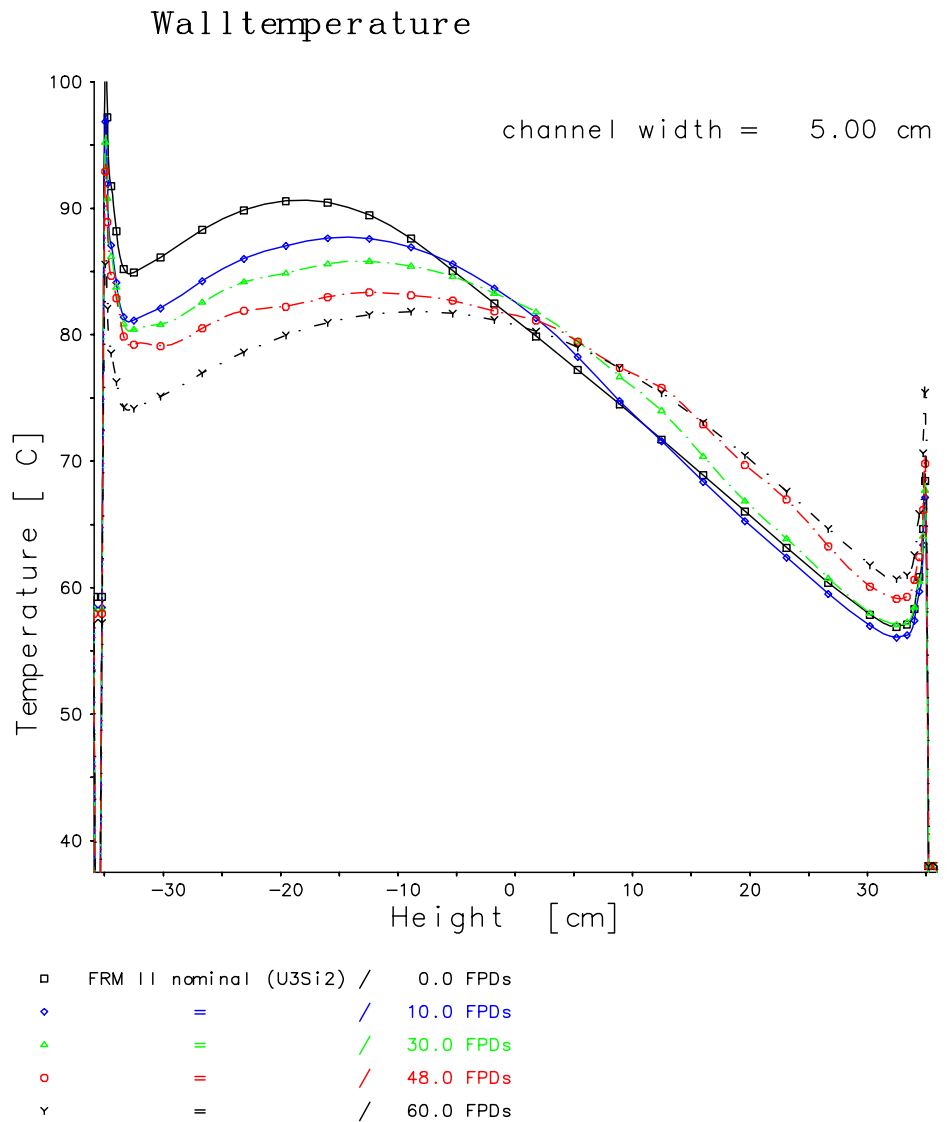
FRM II nominal (U3Si2), density splitting, 93% enriched
neutronics/thermohydraulics: DIFF2D/NBK 53*64/30*34 meshes
cycle at 20.0MW: 60.0 FPDs, flow speed in channel: 17.5 m/s

Walltemperature

	Height =	−33.00 cm		Y	Height =	33.00 cm
◇	Height =	−20.00 cm		×	Height =	20.00 cm
△	Height =	−10.00 cm		*	Height =	10.00 cm
○	Height =	0.00 cm				

Next is shown the timely evolution of the temperature profile of the hot fluid element at a width in the channel of 5.0 cm (compare last Fig. 3):

- NBK calculated the absolute maximum values to lie at the bottom borders over an extent of the plates of only some mm (height =-35cm in Fig. 4). But this is not fairly true when respecting also the axial heat transfer in the plates, which cannot be neglected at the plate ends.

  The description of NBK shows the typical effect of heat transfer in the plates at the meat edge, where a clear local maximum in the power distribution occurs over a few mm only. The peak is fairly drawn down and in the actual case it will be not higher than the broad maximum value inside at the plate surface. This can also be conformed by plausibility considerations.

- At reactor start the power in the inner core region is shoved down by the CR being present above -7 cm (relative to the core mid plane CMP). The hottest point at the plates is located down at about -20 cm and reaches slightly more than 90°C.

- With operation time during a cycle the hottest point at plates surface moves up more to the CMP and becomes clearly cooler, about 80°C till the operations end at 60 FPDs. The CR is then nearly totally removed and the power density is rather symmetrically around the CMP, although the temperatures remain higher at the bottom side, since the coolant water comes from the top.

Fig. 4:
Timely evolution of the temperature profile of the hot fluid element at a width in the channel of 5.0 cm (compare Fig. 3) at the surface of the typical fuel plate of FRM II over the extended cycle of 60 days (full power operation at 20 MW).
At BOC the power in the inner core region is shoved down with the CR being present above -7 cm. At EOC the CR is nearly totally removed and the power density is rather symmetrically around the CMP, although the temperatures remain higher at the bottom side, since the coolant water comes from the top.

Walltemperature

channel width = 5.00 cm

□	FRM II nominal (U3Si2) /	0.0 FPDs	
◇	= /	10.0 FPDs	
△	= /	30.0 FPDs	
○	= /	48.0 FPDs	
Y	= /	60.0 FPDs	

SUMMARY / OUTLOOK

This work establishes the timely evolution of the surface temperatures of FRM II fuel plates. One can derive a time averaged maximum temperature that is clearly lower than established for cycle start at any safety contemplation for FRM II. The maximum value is in time average not higher than 85°C even when taking some conservative values for the coolant conditions. For the conversion of FRM II this can be helpful in case the fuel of final selection exhibits an obvious temperature dependence at irradiation tests that cover the maximum wall temperature range of FRM II plates up to about 100°C.

REFERENCES

[1]   Proceedings of "International Meetings on Reduced Enrichment for Research and Test Reactors RERTR-2006", Cape Town, South Africa, several contributions therein.

[2]   "Reduced enrichment program for FRM II, status of 2006", 11th International Topical Meeting on Research Reactor Fuel Management, RRFM 2007, Lyon, A. Röhrmoser, W. Petry

[3]   "Reduced enrichment program for FRM II, actual status & a principal study of monolithic fuel for FRM II", 10th International Topical Meeting on Research Reactor Fuel Management, A. Röhrmoser, W. Petry, RRFM 2006, Sofia

[4]   "Test Irradiations of Full Sized U3Si2-Al Fuel Plates up to Very High Fission Densities", K. Böning, W. Petry, 2008, Journal of Nuclear Materials

[5]   "Investigations on the cooling of a compact core for a research reactor", A. Röhrmoser, diploma thesis at TU Munich, 1984

[6]   "Investigations on the cooling of a compact core with involute fuel plates", Chr. Döderlein, thesis at TU Munich, written in German, 1989

[7]   "Safety report for High flux reactor RHF", Volume 4, Institute Laue-Langevin, ILL, Grenoble 1972

UPSCALING CABRI CORE KNOWLEDGE FOR A NEW SAFETY CASE

J. ESTRADE, G. RITTER
CEA/Direction de l'Énergie Nucléaire/DER/SRES.
B^t 721. Cadarache, 13108 St Paul Lez Durance, FRANCE

D. BESTION
CEA/Direction de l'Énergie Nucléaire/DER/SSTH.
B^t 501. 17, Av. des martyrs. 38054 Grenoble, FRANCE

J-CH. BRACHET
CEA/Direction de l'Énergie Nucléaire/DMN/SRMA.
B^t 357. 91191 Gif sur Yvette, FRANCE

Y. GUÉRIN
CEA/Direction de l'Énergie Nucléaire/DEC/SESC.
B^t 151. Cadarache 13108 St Paul Lez Durance, FRANCE

O. GUÉTON
CEA/Direction de l'Énergie Nucléaire/DER/SPRC.
B^t 238. Cadarache 13108 St Paul Lez Durance, FRANCE

ABSTRACT

The CABRI experimental reactor is located at the Cadarache nuclear research center, southern France. It has been successfully operated by CEA during the last 30 years, enlightening the knowledge of FBR and LWR fuel behaviour during RIA and LOCA transients. This operation was interrupted in 2003 to allow for a whole facility renewal programme. The main goal of this reconstruction project is to meet thermal hydraulics parameters identical to LWR standard and downgraded conditions. For this, the sodium cooled experimental loop is now being replaced by a pressurized water loop.

In addition, several key safety issues of the facility have been revisited in order to defend a comprehensive safety case before the safety authority. First item in the case is of course the core. The aim of this paper is to present the path leading to a new core operations domain through expertise, mechanical tests and numerical computations.

The project is funded by IRSN through the CABRI International Programme (CIP) framework.

1.   Introduction

The CABRI facility is made of a pool type reactor in which a dedicated pressurized water loop allows to control phenomena relevant to the single experimental rod during the transient. The core is basically a neutron oven, generating fissions in the experimental rod located in its centre. A vertical channel symmetrical across the core allows the hodoscope, a unique neutron digital camera, to monitor the course of fissions in the experimental rod along the experiment.

The core is made of 1488 stainless steel clad fuel rods with a 6% 235U enrichment. These rods are inserted in 5 types of sub-assemblies. The reactivity is controlled via 6 bundles of 23 Hf rods.
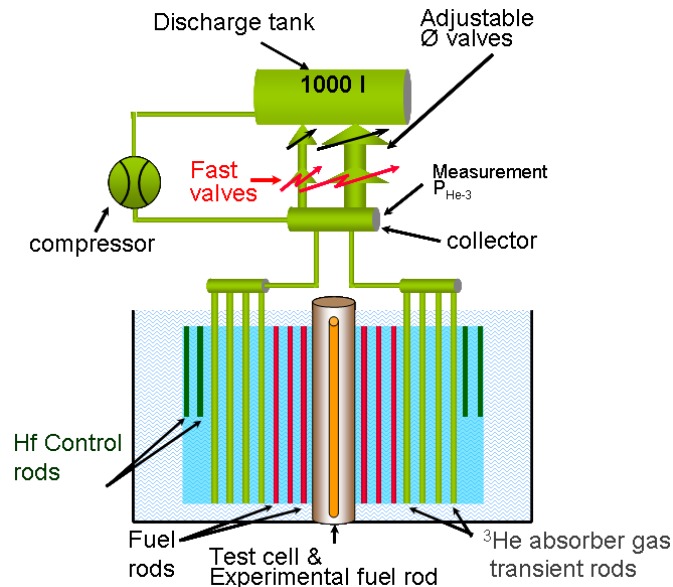

Fig 1. Principle of operation of the CABRI facility

Eventually, the key feature of the CABRI core is its reactivity injection system.

This device allows 96 tubes filled with 3He (major neutron absorber) up to a pressure of 15 bars and located among fuel rods to depressurize very fast in a discharge tank. The absorber ejection translates into an equivalent reactivity injection possibly reaching 4$ within a few 10ms. The power consequently bursts from 100 kW up to ~20GW in a few ms and decreases just as fast due to the Doppler effect and other delayed reactivity feed-backs. The experimental simulation of RIA the CABRI core provides to the experimental rod is of course also withstood by the driver core fuel rods.

This feed core fuel rods were designed in the early 1970's to operate in these very demanding conditions.

The facility renewal programme started in 2003 allowed for sharp examination of core fuel rods which revealed a local and partial fusion in one of the hot rods. A level 1 incident was declared to the safety authority. The up scaling of the CABRI core safety case had just started.

2. A new domain for operation

The allowed domain for operation was determined both by a maximum fuel temperature and a maximum heat flux to the coolant. These criteria were not coherent with actual core operating conditions and thus were replaced by a new set of limits. The features now describing the core fuel rod behaviour are the clad maximum temperature and strain as well as the fuel maximum temperature. The new domain for operation (cf. fig. 2) is now consistent with the confinement function allocated to the core fuel rod cladding.
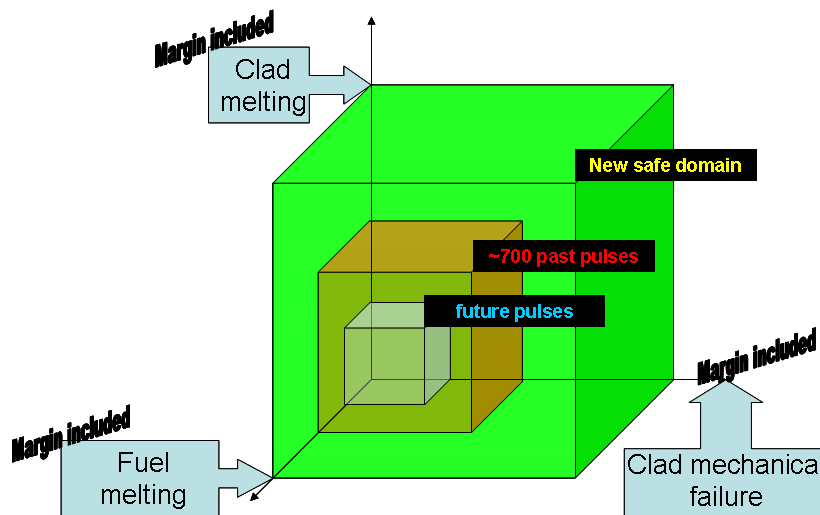
Fig 2. New domain for operation

3. Validation of core behaviour through expertise, dedicated experiments and numerical computations

Understanding past CABRI experimental programmes

After that the evidence of a local fusion was uncovered, a comprehensive analysis was started to analyse the cause of this event. The investigation included destructive rod examinations, a full characterization of fuel pellets and a very large programme of computational simulations of past experiments according to three key viewpoints. The study was based on cutting edge thermal hydraulics, reactor physics and mechanics. According to this enquiry the fusion event seems to have occurred during a ramp type of test. This type of test will not be performed anymore in the future.

Safety assessment for future experimental programmes

The ability to meet past experimental conditions by numerical simulation was a first step towards proving the control of future programmes. An additional mechanical tests campaign was conducted onto the clad of used and fresh rods. The goal of this operation was to determine maximum stress conditions for the clad. It thus allowed defining the maximum tolerable strain and temperature in the clad. The numerical simulation action launched to understand the past was also extended to demonstrate the capacity to meet experimental objectives while remaining within a safe perimeter. The thermal hydraulics models were validated in that perspective on a set of experiments typical of CABRI conditions. Eventually, the hot rod behaviour during future CABRI like tests was computed according to best estimate and conservative hypotheses. It showed future experiments would not take the rods beyond the safety domain.

4. Commissioning the facility for the upcoming CIP series

Re-starting CABRI after 6 years without experiments will come up through a dedicated procedure. All core physics features will be tested step by step, bottom up, until full confidence is acquired on the safety of the facility. The main characteristics will be validated during two key phases, i.e. neutron commissioning and power commissioning, described hereafter.

Neutron commissioning

During these tests the reactivity will be monitored in a static mode either by control rods level difference or by ^{3}He pressure difference. The integral and differential rods and ^{3}He reactivity worth will be measured. An attempt to monitor slow dynamics reactivity feedbacks like moderator or coolant effect should be initiated. But also during the power bursts an effort will be dedicated to retrieve an assessment of the Doppler effect. Eventually, the main parameters to be measured in CABRI are of course the weight of delayed neutrons and the neutron lifetime β and l.

Power commissioning

The absolute power module will be measured at medium power by a usual heat balance. This will allow the calibration of experimentalists and facility operators ion chambers. During the power burst and as there can be no heat balance at such a power level, it will be necessary to rely also on an integration methodology corresponding to a dosimetry experiment. This power integration will be compared to the energy integrated by the ion chambers during the peak of power. The coupling between core and experimental rod should be determined through a set of dosimetry measurements. The nature and location of dosimeters should be optimized in order to assure the best measurement.

The last phase of power commissioning will proceed through a progressive pattern in order to remain conservatively within the new safe operations domain. This so-called start-ups phase will consist in power bursts initiated by the reactivity insertion system. The key parameters of this device are the ^{3}He pressure and the ^{3}He valves aperture, respectively determining the maximum injected reactivity and the maximum injection rate. In that perspective, these crucial factors will be increased stepwise from ❶ to ❾ as in figure 3.
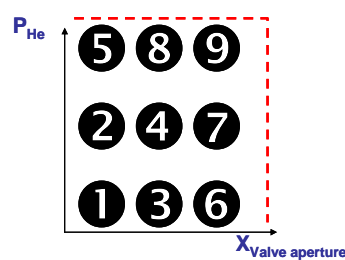

Fig 3. Experimental start-ups commissioning pattern

5. Conclusion

This paper presents how the CABRI core safety case was upgraded. It introduces past and future operation domains. It also reminds how the understanding of the past presented the conditions leading to a partial and local fusion event. Eventually, the assessment of the core fuel rods behaviour during the future experimental programme through numerical simulations showed it would remain well within a safe perimeter.

When the core is ready to start commissioning under standard conditions, all possible parameters will be progressively checked while in operation to make sure that pre-test safety assessments were correct.

European Nuclear Society

Rue Belliard 65
1040 Brussels
Belgium
Telephone +32 2 505 30 54
Fax + 32 2 502 39 02

rrfm2009@euronuclear.org

www.euronuclear.org

IAEA
International Atomic Energy Agency

ATOMINSTITUT

TU
W I E N